

# IMAGE PROCESSING TO OPTIMIZE WAVE ENERGY CONVERTERS

A thesis presented to the faculty of the Graduate School of  
Western Carolina University in partial fulfillment of the  
requirements for the degree of Master of Science in Technology.

By

Kyle Marc-Anthony Bailey

Director: Dr. Peter C. Tay  
Associate Professor  
Department of Engineering and Technology

Committee Members:

Dr. H. Bora Karayaka, Department of Engineering and Technology  
Dr. Yanjun Yan, Department of Engineering and Technology

April 2016

©2016 by Kyle Bailey

This thesis is dedicated to my parents.

Age Quod Agis!

## ACKNOWLEDGEMENTS

I would like to thank my advisor, Dr. Peter C. Tay, he is an inspiration and a great mentor. He has been my go to professor here at Western Carolina University for the past six years. Without his guidance, support and expertise none of this would've been possible. He is always willing to help and goes the extra mile when it comes to supporting students.

I would also like to thank my committee members, Dr. H. Bora Karayaka and Dr. Yan for their constant support and extensive knowledge. Lastly, I would like to thank my colleagues in the Master of Science Technology program, having the opportunity to brainstorm and discuss with them has been a great help in accomplishing this thesis.

## TABLE OF CONTENTS

LIST OF TABLES .....	v
LIST OF FIGURES .....	vi
ABSTRACT .....	vii
CHAPTER 1: INTRODUCTION .....	8
1.1 Digital Images .....	8
1.2 Sampling .....	9
1.3 Subband Decomposition .....	9
CHAPTER 2: BACKGROUND .....	10
CHAPTER 3: METHODOLOGY .....	16
CHAPTER 4: RESULTS AND DISCUSSION .....	19
CHAPTER 5: CONCLUSION .....	33
Bibliography .....	34
Appendices .....	35
APPENDIX A: High Resolution Energy Tables .....	36
Appendix B: Source Codes .....	60

## LIST OF TABLES

Table 4.1: Energy of simulated images.....	20
Table 4.2: Excerpt showing Energy of Bermuda.....	24
Table 4.3: Excerpt showing Energy of Nishinoshima .....	27
Table 4.4: Excerpt showing Energy of Palau.....	30
Table 4.5: Excerpt showing Energy of Townsville .....	32
Table A. 1: Energy of Bermuda.....	36
Table A. 2: Energy of Nishinoshima .....	42
Table A. 3: Energy of Palau.....	48
Table A. 4: Energy of Townsville.....	54

## LIST OF FIGURES

Figure 2.1: Response due to $\cos(2\pi f_1 n)$ where $f_1.$ is in SB1.....	12
Figure 2.2: Energy Calculation .....	13
Figure 2.3: Magnitude Response with White Gaussian Noise .....	13
Figure 2.4: Energy of White Gaussian Noise .....	14
Figure 2.5: Magnitude Response with Uncorrelated Random Noise .....	14
Figure 2.6: Energy with Uncorrelated Random Noise.....	15
Figure 4.1: Low Resolution Image of Bermuda with scale .....	22
Figure 4.2: High resolution satellite image of Bermuda with ROI.....	22
Figure 4.3: Bermuda's enlarged Region of Interest.....	23
Figure 4.4: Crop Image of Nishinoshima with scale .....	25
Figure 4.5: High Resolution Image of Nishinoshima with ROI .....	26
Figure 4.6: Nishinoshima's enlarged Region of Interest .....	26
Figure 4.7: Full field image of Palau.....	28
Figure 4.8: Enlarged cropped sub-image enclosed by the white box in Figure 4.7.....	28
Figure 4.9: High resolution satellite image of Palau with ROI.....	29
Figure 4.10: Palau's enlarged Region of Interest.....	29
Figure 4.11: Cropped Image of Townsville with scale.....	31
Figure 4.12: Satellite Image of Townsville with ROI.....	31
Figure 4.13: Townsville's enlarged Region of Interest .....	32

## ABSTRACT

### IMAGE PROCESSING TO OPTIMIZE WAVE ENERGY CONVERTERS

Kyle Marc-Anthony Bailey, M.S.T.

Western Carolina University (March 2016)

Director: Dr. Peter C. Tay

The world is turning to renewable energies as a means of ensuring the planet's future and well-being. There have been a few attempts in the past to utilize wave power as a means of generating electricity through the use of Wave Energy Converters (WEC), but only recently are they becoming a focal point in the renewable energy field. Over the past few years there has been a global drive to advance the efficiency of WEC. Placing a mechanical device either onshore or offshore that captures the energy within ocean surface waves to drive a mechanical device is how wave power is produced. This paper seeks to provide a novel and innovative way to estimate ocean wave frequency through the use of image processing. This will be achieved by applying a complex modulated lapped orthogonal transform filter bank to satellite images of ocean waves. The complex modulated lapped orthogonal transform filterbank provides an equal subband decomposition of the Nyquist bounded discrete time Fourier Transform spectrum. The maximum energy of the 2D complex modulated lapped transform subband is used to determine the horizontal and vertical frequency, which subsequently can be used to determine the wave frequency in the direction of the WEC by a simple trigonometric scaling. The robustness of the proposed method is provided by the applications to simulated and real satellite images where the frequency is known.

## CHAPTER 1: INTRODUCTION

Wave Energy Conversion (WEC) is the process of harnessing the ocean's power and converting it into electricity [1]. Since ocean waves are constantly moving, this motion can be used to turn a slider crank mechanism [1]. By sending this mechanical motion through a generator, electrical current can then be generated. WECs need extensive coastal access in order to be sustainable. The top three WEC farms in the world right now are located in Australia, Portugal and the United Kingdom. All three of these countries have massive amounts of coastal access and this makes them great areas for WEC farms. WECs are also one of the least intrusive forms of renewable energy. They don't create any environmentally hazardous waste, nor do they emit CO<sub>2</sub>. This is good since there has been a focus in protecting our earth and sustaining it for generations to come.

In order to maximize the amount of energy a WEC can generate, they need to be optimized the frequency, amplitude and shape of the incoming or existing wave [1]. Once this information is attained the WEC can then be tuned to achieve maximal energy generation. This thesis will focus on determining an effective method to estimate the frequency of ocean waves—from satellite images.

### **1.1 Digital Images**

Digital Images are composed of an array of pixels. For example, a size 6000 x 4800 digital image is composed of 6000 rows by 4800 columns of picture elements. Each picture element (pixel) location is indexed by the row number and the column number. Each pixel is also composed of three 8 or more bit integers for color images and only one 8 or more-bit integer for black and white images. The three color integers values represent the amount of red, green and blue (RGB) light that is detected by a two dimensional (2D) array of charged coupled devices (CCD),

complementary metal-oxide semiconductors (CMOS), or other visible light sensors. It is simple arithmetic (weighted sum of RGB values) to convert color images to a grayscale image. The conversion from grayscale to color is not as straight forward and still an open ended research topic.

## 1.2 Sampling

The digital image size in pixels and actual area (kilometer squared ( $\text{km}^2$ )) determine the sampling frequency,  $f_s$ . Throughout this thesis, I am assuming that the horizontal  $f_s$  is the same as the vertical  $f_s$ . The Nyquist Shannon Theorem [3] guarantees that analog frequencies within plus and minus  $\frac{f_s}{2}$  are accurately captured in the sampling process. Frequencies outside of  $[-\frac{f_s}{2}, \frac{f_s}{2}]$  produce aliases to some frequency within  $[-\frac{f_s}{2}, \frac{f_s}{2}]$ .

## 1.3 Subband Decomposition

Since the images used in this thesis will be restricted to real valued pixels, the discrete time Fourier transform (DTFT) complex values within  $[-\frac{f_s}{2}, 0]$  will be complex conjugate mirror about the vertical axis of the DTFT values within  $[0, \frac{f_s}{2}]$ . In this thesis, I propose to divide the frequency interval  $[0, \frac{f_s}{2}]$  into L many equal subbands. To accomplish the subband decomposition, I propose convolving the digital image with an optimally frequency localized L-channel CMLT filterbank. The frequency optimization of the CMLT filterbank is beyond the scope of this thesis. In this regards I rely on my thesis advisor, Peter C. Tay's expertise in filterbank construction.

## CHAPTER 2: BACKGROUND

A maximally decimated perfect reconstruction filterbank (MDPRF) is a filterbank that has the minimum sample rates for its subbands, which would be twice the Nyquist frequency [3]. The modulated lapped transform (MLT) provides an easy method to implement a L-channel MDPRF. The perfect reconstruction aspect of the MLT is potentially important in that perfect reconstruction ensures no loss of information, since the original signal or image can be reconstructed from the output of the subband analysis decomposition. The MLT has several filters and the length of those filters is twice that of the channels,  $2L$ . The way this process was implemented was first to define the number of intended channels. In the case of this experiment, seven channels were selected. Each channel for the filter is twice the length of the channel, resulting in  $2L=14$ . The complex modulated lapped transform (CMLT) is defined as

$$h_k[n] = \sqrt{\frac{2}{L}} \omega[n] m_k[n] \quad (1)$$

where

$$m_k[n] = \cos\left[n + \frac{2L+1}{2} \left(k + \frac{1}{2}\right) \frac{\pi}{2L}\right]$$

And  $n=0,1,2,\dots,2L-1$ .

The MLT can then be extended into complex values by allowing the modulating function to be:

$$m_k[n] = e^{j\left[n + \frac{2L+1}{2} \left(k + \frac{1}{2}\right) \frac{\pi}{2L}\right]}.$$

The perfect reconstruction is critical in the design and determined only by the values of  $\omega[n]$ . Each channel of the CMLT, is able to detect sinusoidal frequencies in a certain range, thus

the sampling frequency  $f_s$  and maximum frequency  $f_{\max}$  needs to be calculated. In order to determine the maximum frequency, one simply divides the sampling frequency by two,  $f_{\max} = \frac{f_s}{2}$ .

The bandwidth also needs to be calculated due to the fact that the filterbank splits the frequency range  $[0, f_{\max}]$  into  $L$  subbands. This was achieved by dividing the maximum frequency by  $L$ ,

$$BW = \frac{f_{\max}}{L}.$$

The filter  $h_i$  from equation (1) represents a filter in the MLT or CMLT, with a frequency subband range of  $SB_i = [i \times BW, (i + 1) \times BW]$  for  $i = 0, 1, 2, \dots, L - 1$ . Therefore any frequency within this range,  $SB_i$ , will pass through the filterbank, and a frequency outside of that range will be mostly eliminated.

The following function is an example of the input into the MLT filterbank

$$x(n) = \cos(2\pi fn)$$

where  $n = 0, 0.01, 0.02, \dots, 3$ ,  $f = 1.5 (\frac{f_{\max}}{7})$  and  $f_{\max} = 50\text{Hz}$ . Figure 2.1 shows the squared magnitude response of this example input. The subband with the maximum energy,  $E_{\max} = \max \{E_i\}$  where

$$E_i = \sum_n |x(n) * h_i(n)|^2,$$

is used to estimate the wave frequency. It can be observed based on Figure 2.1 that  $SB_1$  or channel 1 (channels range from 0 - 6). is where the energy is concentrated.

Two types of noise were added to the signal in order to show how noise affected the accuracy of the estimation; firstly, white Gaussian noise (Figure 2.3) and then uncorrelated random noise (Figure 2.5). Adding up the magnitude for each channel and then displaying them, giving a clear numerical value, then determining the maximum energy for each channel. Upon examining Figure 2.2, Figure 2.4, and Figure 2.6 one can determine that the maximum energy is concentrated

in  $\text{SB}_1$ . The true energy estimation of 5.8693 (Figure 2.2) is thrown off greatly by the addition of noise, so much so that our precise estimation has become that of 7.9451 (Figure 2.6). The noise is adding energy to each channel and in doing so throws off the estimation. This shows that this is a reliable method to decompose signals and it also provides a robust estimate of wave frequency.

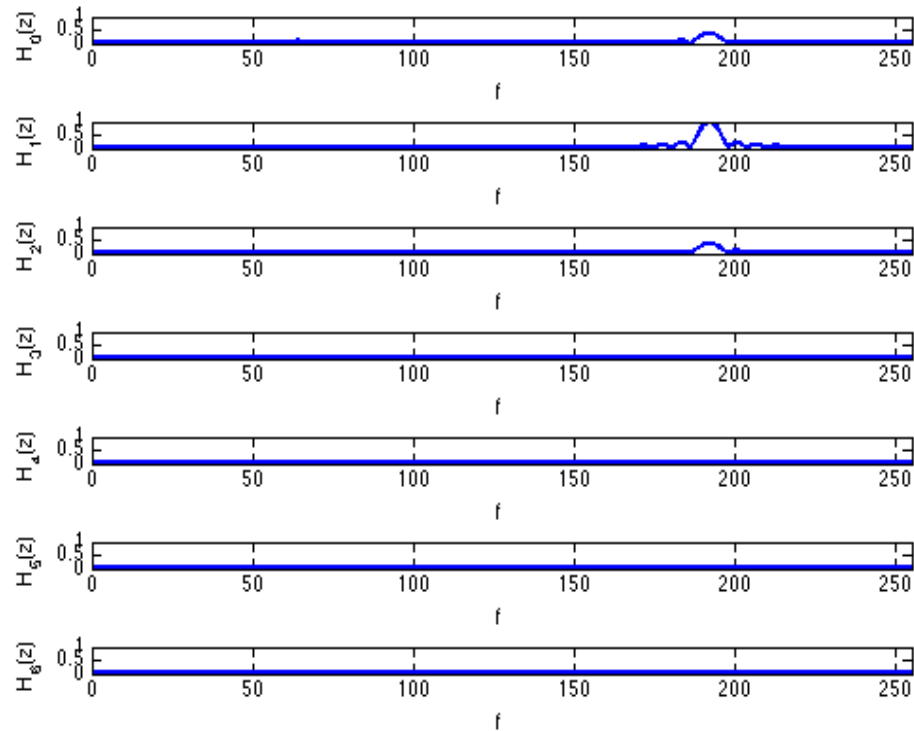


Figure 2.1: Response due to  $\cos(2\pi f_1 n)$  where  $f_1$  is in  $\text{SB}_1$ .

### Command Window

```
>> t=0:0.01:3;
x=cos(2*pi*(50/7)*1.5*t);
load('FB_7channel_best_freq_localized.mat')
[energy,y]=fb_decomposition(t,x,w);
>> energy

energy =
0.8901
5.8693
0.8583
0.0369
0.0034
0.0025
0.0022
```

Figure 2.2: Energy Calculation

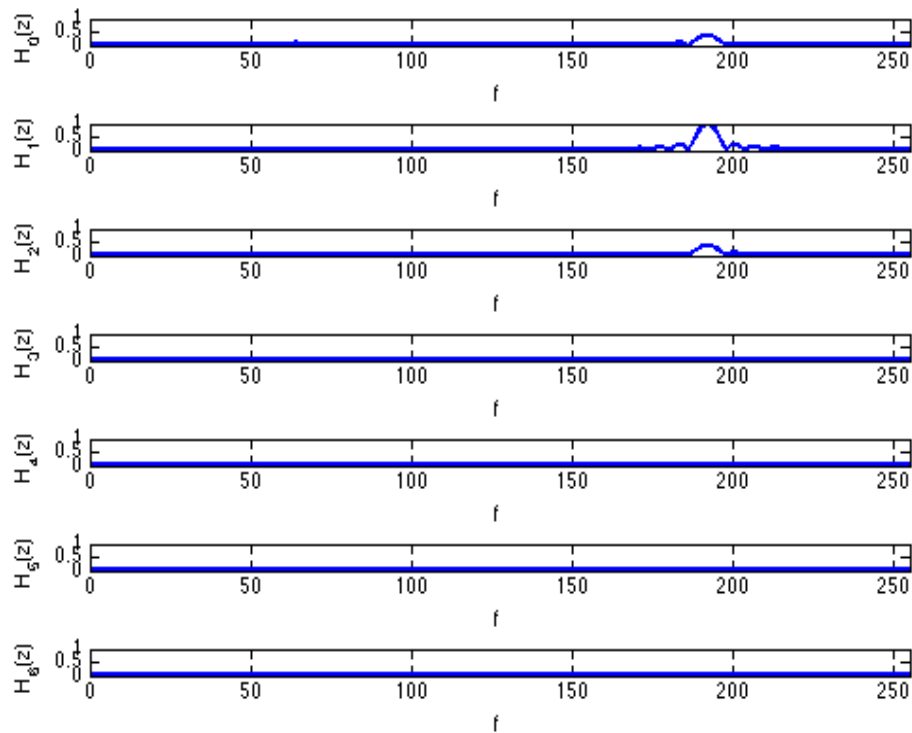


Figure 2.3: Magnitude Response with White Gaussian Noise

### Command Window

```
>> t=0:0.01:3;
x=cos(2*pi*(50/7)*1.5*t)+awgn(x,10,'measured');
load('FB_7channel_best_freq_localized.mat')
[energy,y]=fb_decomposition(t,x,w);
>> energy

energy =

0.9424
5.9367
0.9252
0.0929
0.0684
0.0550
0.0507
```

Figure 2.4: Energy of White Gaussian Noise

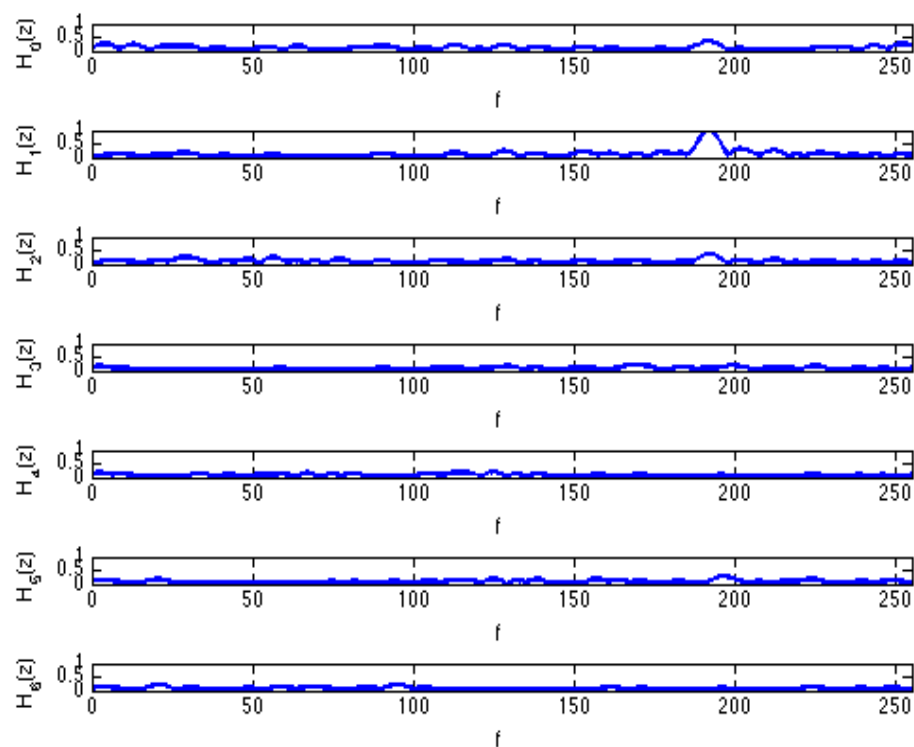


Figure 2.5: Magnitude Response with Uncorrelated Random Noise

### Command Window

```
>> t=0:0.01:3;
x=cos(2*pi*(50/7)*1.5*t)+randn(1,length(t));
load('FB_7channel_best_freq_localized.mat')
[energy,y]=fb_decomposition(t,x,w);
>> energy

energy =

    3.2182
    7.9451
    2.7224
    1.5143
    1.8781
    1.9767
    1.7509
```

Figure 2.6: Energy with Uncorrelated Random Noise

## CHAPTER 3: METHODOLOGY

By taking each row of an image ( $I$ ) and each column of an image ( $I$ ) and convolving it respectively with a 1D filter, a 2D filter can be created. This is a separable extension of a 1D filter into a 2D filter, denoted by

$$H_{l,k}(n, m) = h_l(n) * h_k(m). \quad (3)$$

This method is commutative, which means  $H_{l,k} = H_{k,l}$ . The resulting output image ( $I$ ) is represented as

$$\begin{aligned} I_{l,k}(n, m) &= H_{l,k}(n, m) * I(n, m) \\ &= h_k(n) * \forall_m [h_l(m) * \forall_n I(n, m)]. \end{aligned} \quad (4)$$

Similarly, the 2D CMLT can also be expanded which allows it to find a solution to image frequencies, this is carried out by making trigonometric adjustments to the subbands.

$$SB_{l,k} = [l \times BW_r, (l + 1) \times BW_r] \times [k \times BW_c, (k + 1) \times BW_c] \quad (5)$$

The bandwidth along the rows and columns in equation 2 are represented by  $BW_r$  and  $BW_c$  in equation 5. Since the subband with the maximum energy determines the wave frequency, the energy of each subband will also need to be expanded into a 2D filter by applying the following:

$$E_{l,k} = \sum_{n,m} |H_{l,k}(n, m) * I(n, m)|^2. \quad (6)$$

The wave frequency can then be determined by which subband the energy is located in.

This process required high resolution and high quality satellite images so that a wide image frequency bandwidth is captured with adequate signal to noise ratio (SNR). Lower resolution and quality images are compressed, which can reduce SNR and can only represent a smaller frequency

bandwidth than high resolution images. The satellite images, used in the experiment, were acquired from NASA's observatory database and usually provided two versions of the image, a high resolution and a low resolution image. However, upon inspection only the low resolution version of the image provided a scale and the scale for each image was in pixels per kilometers (km). Thus the scale of the low resolution version of the images had to be upscaled accordingly in order to properly utilize the high resolution image.

The low resolution image was read into Matlab, and using the pixel region tool, the pixel values (x and y coordinates) for the left-most end of the scale and the right-most end of the scale were acquired. The difference between these pixel values determined the sampling frequency per km,  $f_s$ , for the low resolution image. Since the low resolution images are just a downsampled version of the high resolution image, it was an easy task (simply multiply the lower resolution  $f_s$  by the upsampling factor) to determine the high resolution sampling rate. By taking the dimensions of each the low resolution and high resolution images, the value at which the images were downsampled can be determined.

For this study, I assumed that the vertical  $f_s$  is the same as the horizontal  $f_s$ . This is due to the fact that the scale provided on the low resolution images ran only from left to right, i.e. horizontally. So the value that was actually calculated was the horizontal  $f_s$ . The rest of the process followed the steps outlined in chapter two to determine  $f_{max}$  and BW, the only difference being that L was set to 33 since that is the number of subbands being used in the 2D separably extended CMLT filterbank.

In order to determine the wave frequency, the 2D extended CMLT had to be applied to the region of interest (ROI). These ROIs are outlined by a red box, which can be seen in Figures 4.2, 4.5, 4.9 and 4.12. However before sending it through the 2D extended CMLT filterbank for

processing, it first had to be normalized. This was done by subtracting the mean pixel value from the image. The energy consumption values were then tabulated for  $l = 0, 1, 2, \dots, 33$  and  $k = 0, 1, 2, \dots, 33$  and the subband  $, SB_{l,k}$ , with the maximum energy located and highlighted in red. Utilizing  $(SB_{l,k} + 0.5) \times BW$ , where 0.5 represents the center frequency of each channel of the filtering, the values for the horizontal frequency and vertical frequency can be determined respectively.

## CHAPTER 4: RESULTS AND DISCUSSION

The initial process outlined in Chapter 3 was first carried out on simulated images in order to determine which subband the energies were located in. The simulated images comprised of a circular symmetric sinusoidal with varying frequencies. They were created with the following input:

$$I(n, m) = \cos(2\pi f(n + m))$$

where  $n \in \mathbb{Z}$ ,  $f = (i + 0.5)(\frac{f_{\max}}{7})$  and  $f_{\max} = 100\text{Hz}$  for  $i = 0, 1, 2, \dots, 7$ . Table 4.1 shows the energies for each channel of the extended 2D CMLT filterbank [2]. The maximum energy for each simulated image is highlighted in red in order to display which SB the wave frequencies are located in. Since the simulated images were sinusoidal in nature, that is why the energies are located in each diagonal subband. This test confirmed that the energies could be accurately located and that the testing of actual satellite images could then be initialized.

Table 4.1: Energy of simulated images

$I_{0,0}$	0	1	2	3	4	5	6
0	<b>0.1027</b>	0.0371	0.0068	0.0012	0.0012	0.0010	0.0010
1	0.0371	0.0113	0.0026	0.0008	0.0008	0.0010	0.0010
2	0.0068	0.0026	0.0008	0.0008	0.0010	0.0009	0.0009
3	0.0012	0.0008	0.0008	0.0011	0.0009	0.0010	0.0010
4	0.0012	0.0008	0.0010	0.0009	0.0011	0.0010	0.0007
5	0.0010	0.0010	0.0009	0.0010	0.0010	0.0006	0.0006
6	0.0010	0.0010	0.0009	0.0010	0.0007	0.0006	0.0006
$I_{1,1}$	0	1	2	3	4	5	6
0	0.0080	0.0400	0.0314	0.0034	0.0031	0.0031	0.0028
1	0.0400	<b>0.0643</b>	0.0286	0.0052	0.0036	0.0029	0.0025
2	0.0314	0.0286	0.0084	0.0034	0.0023	0.0023	0.0021
3	0.0034	0.0052	0.0034	0.0020	0.0023	0.0021	0.0022
4	0.0031	0.0036	0.0023	0.0023	0.0022	0.0023	0.0032
5	0.0031	0.0029	0.0023	0.0021	0.0023	0.0035	0.0030
6	0.0028	0.0025	0.0021	0.0022	0.0032	0.0030	0.0018
$I_{2,2}$	0	1	2	3	4	5	6
0	0.0027	0.0040	0.0129	0.0229	0.0083	0.0037	0.0026
1	0.0040	0.0068	0.0271	0.0293	0.0069	0.0037	0.0033
2	0.0129	0.0271	<b>0.0412</b>	0.0213	0.0054	0.0040	0.0039
3	0.0229	0.0293	0.0213	0.0084	0.0041	0.0036	0.0032
4	0.0083	0.0069	0.0054	0.0041	0.0031	0.0035	0.0035
5	0.0037	0.0037	0.0040	0.0036	0.0035	0.0035	0.0041
6	0.0026	0.0033	0.0039	0.0032	0.0035	0.0041	0.0067
$I_{3,3}$	0	1	2	3	4	5	6
0	0.0043	0.0040	0.0038	0.0051	0.0145	0.0113	0.0031
1	0.0040	0.0033	0.0045	0.0083	0.0199	0.0115	0.0033
2	0.0038	0.0045	0.0058	0.0183	0.0230	0.0076	0.0040
3	0.0051	0.0083	0.0183	<b>0.0284</b>	0.0165	0.0056	0.0050
4	0.0145	0.0199	0.0230	0.0165	0.0080	0.0054	0.0060
5	0.0113	0.0115	0.0076	0.0056	0.0054	0.0050	0.0098
6	0.0031	0.0033	0.0040	0.0050	0.0060	0.0098	0.0115
$I_{4,4}$	0	1	2	3	4	5	6
0	0.0045	0.0040	0.0041	0.0033	0.0039	0.0079	0.0113
1	0.0040	0.0041	0.0034	0.0036	0.0040	0.0110	0.0136
2	0.0041	0.0034	0.0034	0.0039	0.0060	0.0152	0.0128
3	0.0033	0.0036	0.0039	0.0049	0.0135	0.0179	0.0131
4	0.0039	0.0040	0.0060	0.0135	<b>0.0206</b>	0.0154	0.0142
5	0.0079	0.0110	0.0152	0.0179	0.0154	0.0174	0.0101
6	0.0113	0.0136	0.0128	0.0131	0.0142	0.0101	0.0064
$I_{5,5}$	0	1	2	3	4	5	6
0	0.0045	0.0040	0.0041	0.0033	0.0039	0.0079	0.0113
1	0.0040	0.0041	0.0034	0.0036	0.0040	0.0110	0.0136
2	0.0041	0.0034	0.0034	0.0039	0.0060	0.0152	0.0128
3	0.0033	0.0036	0.0039	0.0049	0.0135	0.0179	0.0131
4	0.0039	0.0040	0.0060	0.0135	0.0206	0.0154	0.0142
5	0.0079	0.0110	0.0152	0.0179	0.0154	<b>0.0174</b>	0.0101
6	0.0113	0.0136	0.0128	0.0131	0.0142	0.0101	0.0064
$I_{6,6}$	0	1	2	3	4	5	6
0	0.0042	0.0043	0.0040	0.0062	0.0159	0.0100	0.0032
1	0.0043	0.0033	0.0045	0.0108	0.0211	0.0096	0.0033
2	0.0040	0.0045	0.0073	0.0223	0.0221	0.0059	0.0039
3	0.0062	0.0108	0.0223	0.0287	0.0141	0.0054	0.0052
4	0.0159	0.0211	0.0221	0.0141	0.0070	0.0052	0.0053
5	0.0100	0.0096	0.0059	0.0054	0.0052	0.0046	0.0084
6	0.0032	0.0033	0.0039	0.0052	0.0053	0.0084	<b>0.0112</b>

The experiment was carried out on four high resolution images: Bermuda, Nishinoshima, Palau and Townsville.

An image of the island of Bermuda, surrounded by the Atlantic ocean [4] was the first of the satellite images for the method detailed in chapter 3 to be implemented upon. The low resolution version of the image, which is 540x720 pixels and shown in Figure 4.1, provided us with a scale of 5km. The  $f_s$  for the low resolution image was 52 samples per 5 km or equivalently  $f_s = 10.4$  samples per km. The high resolution version is shown in Figure 4.2 and the size is 3600x4800 pixels. The upsample by a factor from the high resolution image to the low resolution image is 6.6667, resulting in a  $f_s = 69.3333$  samples per 1km. Also in Figure 4.2 the 512x512 pixel region of interest (ROI) sub-image is shown enclosed in the red box. The ROI is normalized by subtracting the mean pixel value from the image and then applying 2D CMLT [2]. Figure 4.3 shows the 512x512 ROI after conversions from color to grayscale. The energy values were then computed and tabulated. Table 4.2 shows an excerpt of the tabulated results for only  $l = 0, 1, 2, \dots, 4$  and  $k = 0, 1, 2, \dots, 11$ . The complete energy values for  $l = 0, 1, 2, \dots, 33$  and  $k = 0, 1, 2, \dots, 33$  can be seen in Table A.1.

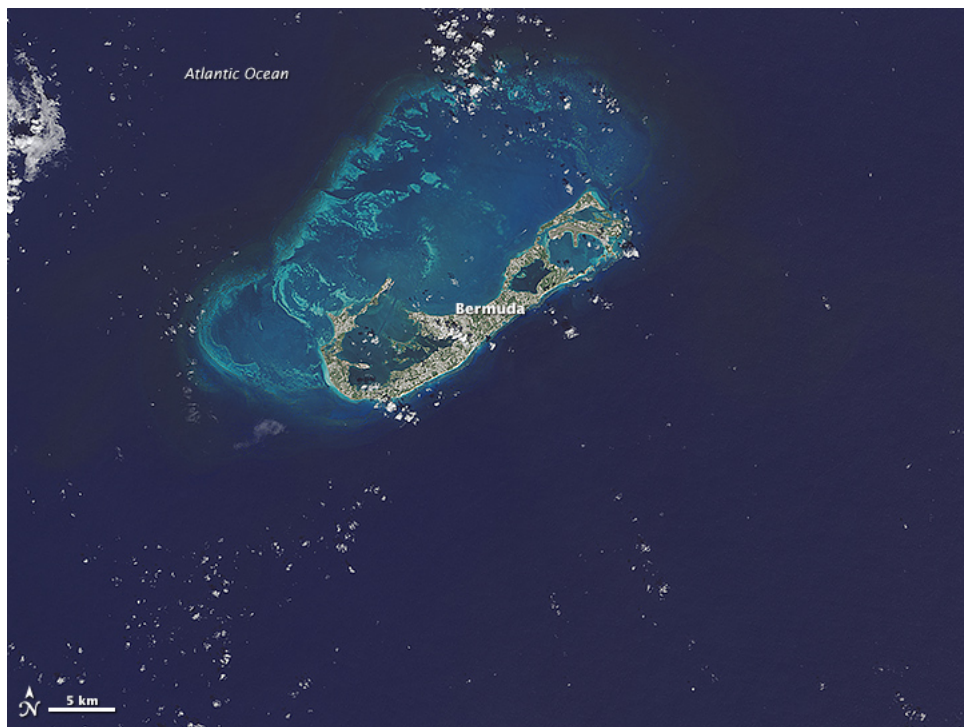


Figure 4.1: Low Resolution Image of Bermuda with scale

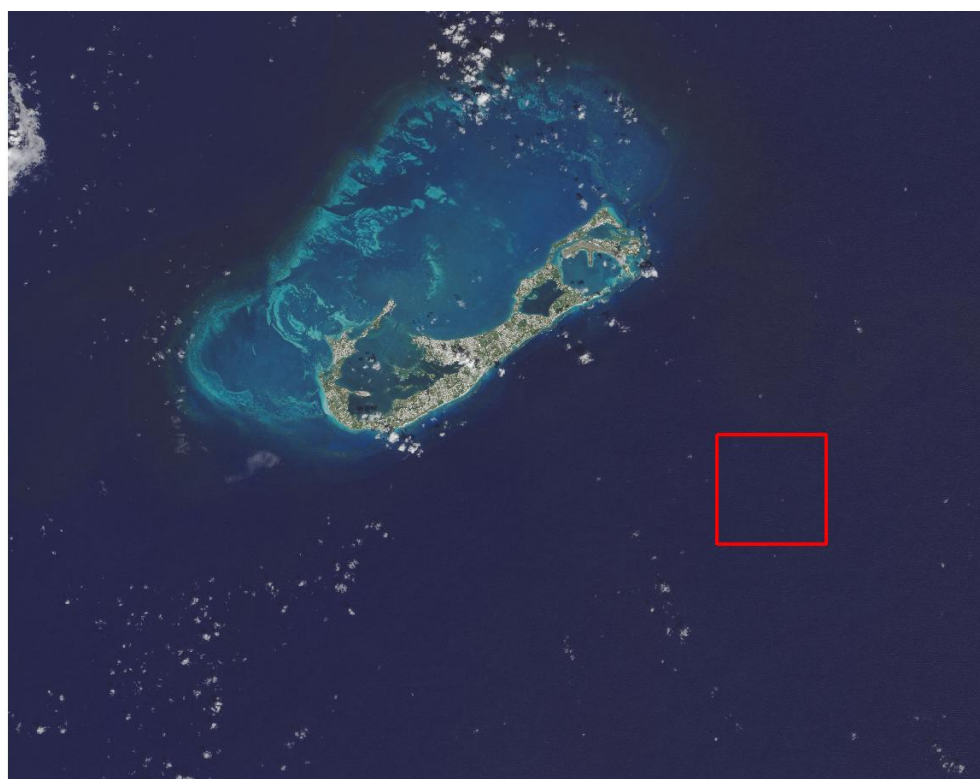


Figure 4.2: High resolution satellite image of Bermuda with ROI

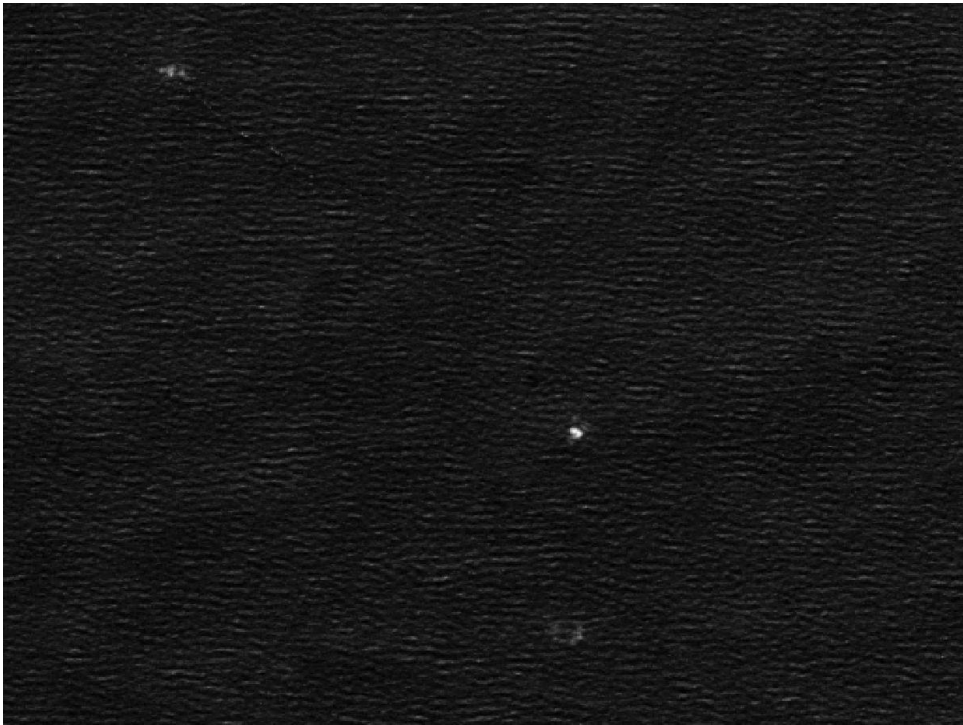


Figure 4.3: Bermuda's enlarged Region of Interest

The maximum energy is highlighted and located in  $E_{0,9}$ . After a 33 channel CMLT 2D separably extend filterbank decomposition, it is determined that the wave frequency energy for Bermuda's ROI is contained in  $SB_{0,9}$ . The resulting horizontal and vertical frequencies are approximately 0.5253 and 9.9798 cycles per km, respectively.

Table 4.2: Excerpt showing Energy of Bermuda

$E_{l,k}$	0	1	2	3	4
0	0.000000	0.006329	0.004151	0.003343	0.002901
1	0.007800	0.004871	0.003810	0.003558	0.003382
2	0.004686	0.004051	0.003996	0.003935	0.003436
3	0.003671	0.003463	0.003829	0.003785	0.003489
4	0.003470	0.003374	0.003361	0.003278	0.003081
5	0.004026	0.004139	0.003613	0.003174	0.003056
6	0.006113	0.006448	0.004930	0.003859	0.003665
7	0.011258	0.010016	0.006737	0.004598	0.004226
8	0.015924	0.012305	0.008062	0.005500	0.004886
9	0.015926	0.011819	0.007915	0.005816	0.004710
10	0.012531	0.010349	0.007664	0.005817	0.004560
11	0.009764	0.009271	0.007512	0.005712	0.004373

The next image to be tested was Nishinoshima [5]. Figure 4.4 depicts the 480x720 pixel cropped image of Nishinoshima with a scale of 1 km. The ROI was selected and depicted in Figure 4.5, enlarged in Figure 4.6. The sampling frequency  $f_s$  for the cropped image was 57 samples per km. Since the image in Figure 4.4 is cropped from the 4871x7306 pixel high resolution image shown in Figure 4.5, the sampling frequency is the same for both the cropped image in Figure 4.4 and the high resolution image in Figure 4.5. Figure 4.5 also shows the ROI sub-image enclosed in the red box. Figure 4.6 shows the grayscale ROI sub-image that is decomposed by the 33-channel 2D CMLT filterbank. An excerpt of the tabulated energy results for only  $l = 0, 1, 2 \dots, 4$  and  $k = 0, 1, 2 \dots, 11$  is displayed in Table 4.3. The maximum energy is located in  $E_{1,8}$  and this tells us that the maximum wave frequency is located in the respective subband,  $SB_{1,8}$ . It was determined that the horizontal frequency and vertical frequency for the high resolution Nishinoshima ROI sub-image was approximately 0.6477 and 3.6705 cycles per km, respectively.

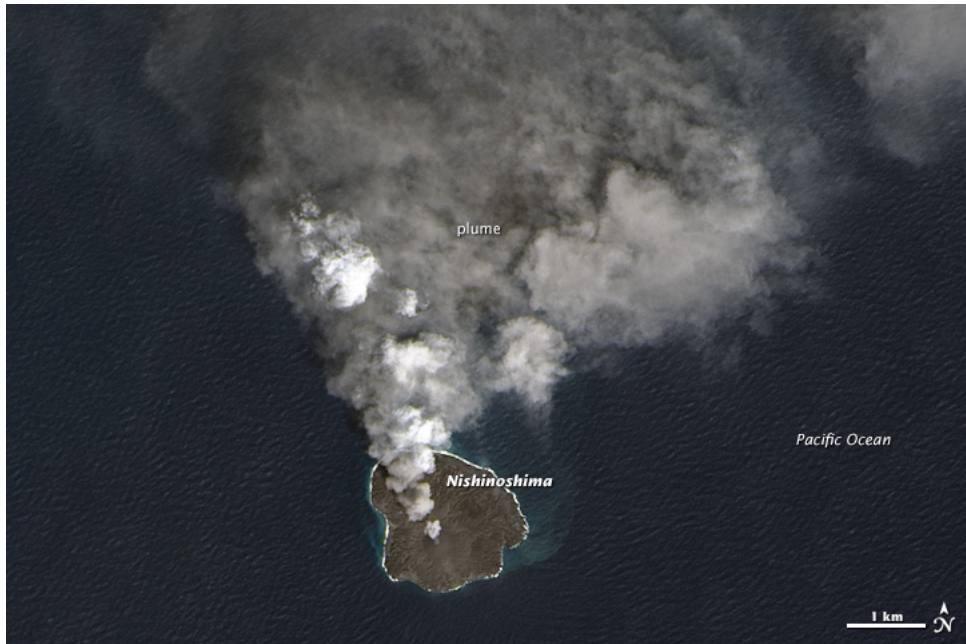


Figure 4.4: Crop Image of Nishinoshima with scale



Figure 4.5: High Resolution Image of Nishinoshima with ROI

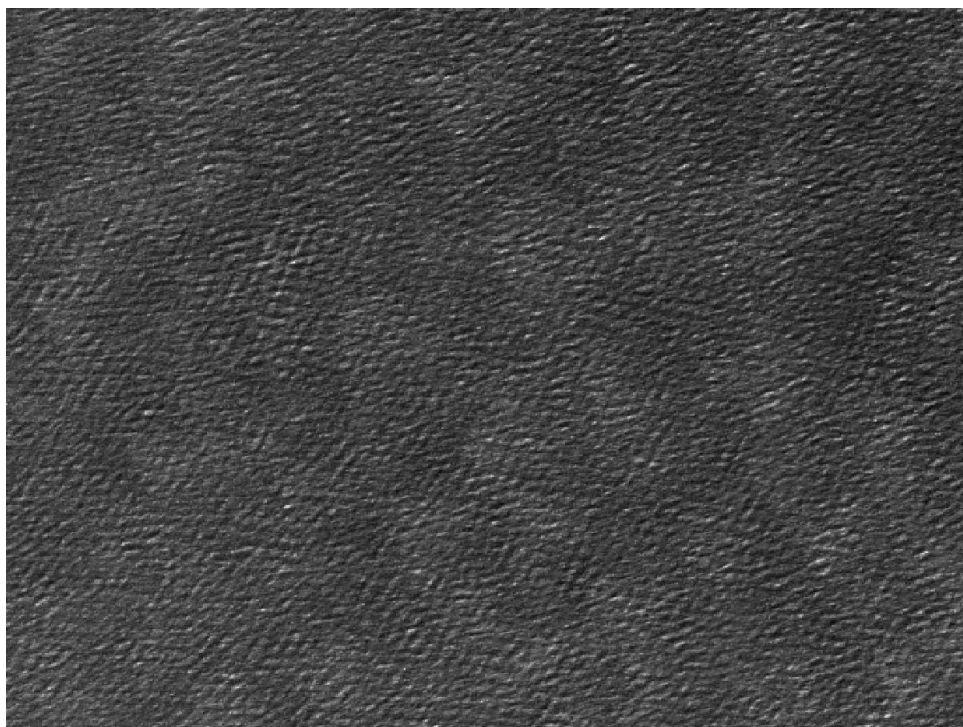


Figure 4.6: Nishinoshima's enlarged Region of Interest

Table 4.3: Excerpt showing Energy of Nishinoshima

$E_{l,k}$	0	1	2	3	4
0	0.000000	0.010621	0.005238	0.004042	0.003719
1	0.008713	0.006466	0.004393	0.003842	0.004163
2	0.004728	0.004069	0.003771	0.003467	0.003694
3	0.003975	0.003822	0.003853	0.004137	0.004680
4	0.004156	0.004041	0.004455	0.005150	0.006901
5	0.005870	0.005675	0.007202	0.007607	0.008727
6	0.008786	0.009198	0.010851	0.011560	0.012349
7	0.011476	0.012859	0.013996	0.014523	0.014136
8	0.012856	0.014904	0.014902	0.014294	0.013328
9	0.011622	0.013238	0.012399	0.011515	0.010894
10	0.009478	0.010267	0.010136	0.010084	0.009079
11	0.007992	0.008534	0.008771	0.008683	0.007949

The 9432x5391 pixel wide field high resolution image of Palau [6] is shown in Figure 4.7.

The white box in Figure 4.7 encloses the cropped 480x720 pixel sub-image, which provides the scale. The cropped sub-image contained in the wide field high resolution image is shown enlarged in Figure 4.8. The cropped sub-images provided a scale that equates 60 pixels to 2 km. Thus the sampling frequency is equal to 30 samples per km,  $f_s = 30$  samples per km for the Palau image. Thus, the maximum resolvable frequency is  $f_{max} = 15$  and the bandwidth of each of the 33 channel CMLT filterbank is  $BW = 0.4545$ . Figure 4.9 shows the ROI that was selected in the high resolution Palau image. Figure 4.10 depicts the enlarged ROI after conversion from color to grayscale pixel values and that was sent through the 33 channel CMLT filterbank. After being processed by the filterbank, the output energy values were tabulated and an excerpt of this is shown in Table 4.4. The maximum energy for the ROI is displayed in  $E_{1,0}$ , which means that the wave frequency is contained in  $SB_{0,1}$ . The horizontal and vertical frequencies contained in the high resolution ROI sub-image were estimated to be 0.2273 and 0.6818 cycles per km, respectively.

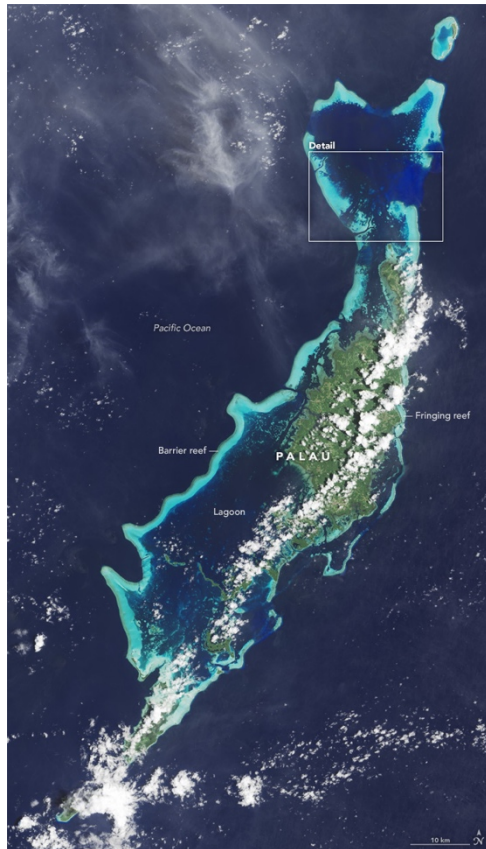


Figure 4.7: Full field image of Palau. The cropped sub-image with scale is enclosed in the white box.



Figure 4.8: Enlarged cropped sub-image enclosed by the white box in Figure 4.7.



Figure 4.9: High resolution satellite image of Palau with ROI.



Figure 4.10: Palau's enlarged Region of Interest

Table 4.4: Excerpt showing Energy of Palau

$E_{l,k}$	0	1	2	3	4
0	0.000000	<b>0.015949</b>	0.010260	0.007064	0.006712
1	0.014344	0.010053	0.006967	0.005747	0.005957
2	0.008337	0.007085	0.005187	0.004636	0.004478
3	0.006414	0.005260	0.004180	0.003916	0.003859
4	0.004773	0.004000	0.003564	0.003335	0.003203
5	0.003251	0.002985	0.002906	0.002904	0.002708
6	0.002538	0.002519	0.002422	0.002657	0.002559
7	0.002030	0.002010	0.002004	0.002236	0.002088
8	0.001908	0.001899	0.001977	0.002021	0.001850
9	0.001733	0.001669	0.001612	0.001640	0.001680
10	0.001586	0.001475	0.001500	0.001513	0.001578
11	0.001425	0.001360	0.001403	0.001331	0.001474

The last image to be tested is an image of a barrier reef off the coast of Townsville, Australia [7]. Figure 4.11 shows the 480x720 pixel high resolution cropped sub-image of Townsville with a scale of 75 pixels equivalent to 2 km. Thus, the sampling rate is  $f_s = 37.5$  samples per km and the maximum frequency,  $f_{max}$ , is one-half  $f_s$ , or equivalently  $f_{max} = 18.75$ . The BW of each 33 channel CMLT filterbank is 0.5682. Figure 4.12 shows the 5448x5448 pixel wide field high resolution image and the 512x512 ROI sub-image that was selected for processing. The ROI sub-image, shown enclose in the red box of Figure 4.12, was sent through the 33 channel CMLT filterbank in order to determining the energies for each respective channel. The energies were tabulated and the maximum energy  $E_{1,0}$  is highlighted. The maximum energy is located in  $E_{1,0}$ . Thus, the maximum wave frequency is located in  $SB_{1,0}$ . The horizontal and vertical frequencies were estimated to be 0.8532 and 0.2841 cycles per km, respectively.

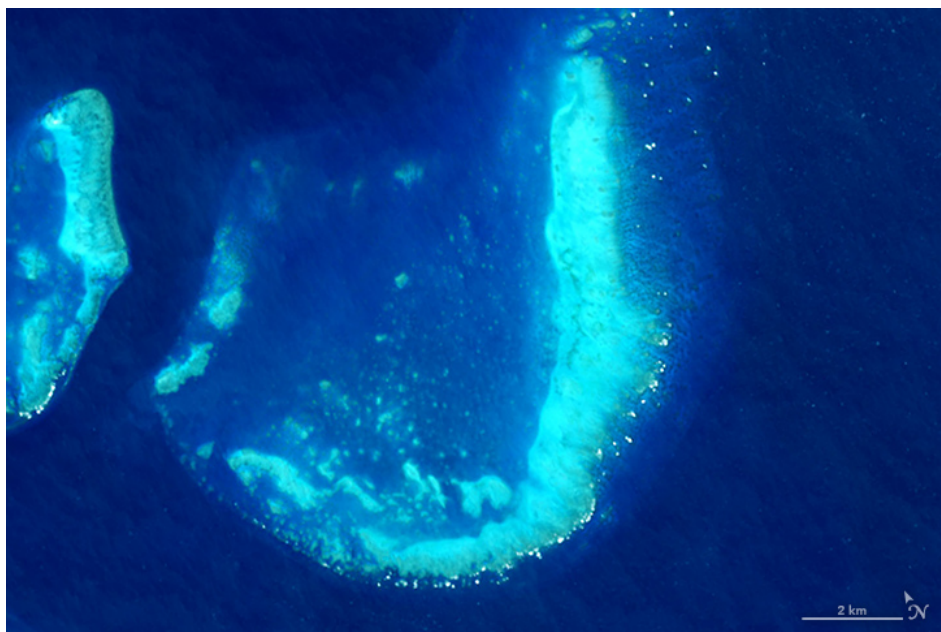


Figure 4.11: Cropped Image of Townsville with scale



Figure 4.12: Satellite Image of Townsville with ROI



Figure 4.13: Townsville's enlarged Region of Interest

Table 4.5: Excerpt showing Energy of Townsville

$E_{l,k}$	0	1	2	3	4
0	0.000000	<b>0.027321</b>	0.016755	0.014807	0.014435
1	0.020946	0.014945	0.013165	0.011121	0.010312
2	0.015298	0.012777	0.012092	0.010133	0.009197
3	0.014857	0.011347	0.010389	0.009576	0.008894
4	0.013387	0.011431	0.010159	0.009887	0.009091
5	0.010452	0.009533	0.009265	0.008745	0.008210
6	0.009386	0.008570	0.009049	0.008070	0.007295
7	0.008615	0.007867	0.008142	0.007160	0.007461
8	0.008131	0.007369	0.007170	0.007017	0.006736
9	0.006885	0.006440	0.006285	0.005727	0.005569
10	0.005683	0.005351	0.005118	0.005057	0.004810
11	0.004815	0.004403	0.004268	0.004097	0.004021

## CHAPTER 5: CONCLUSION

This thesis introduced a way to determine the ocean wave frequency from satellite images using a filterbank method. It provides empirical evidence that using a CMLT filterbank is an effective way of decomposing signals or images into various frequency subbands [1]. It also showed how noise can have an effect on energy estimation. The CMLT filterbank is capable of being separably expanded in order to achieve a 2D multi- channel MDPRF. Since the original input image can be perfectly reconstructed, the multi-channel 2D CMLT filterbank allows for no loss in information throughout the decomposition process. The process outlined in this thesis, using simulated and real visible light satellite images shows that the channel, which exhibits the maximum energy of the output of the analysis CMLT filterbank, provides an accurate estimate of the existing wave frequency. This wave frequency estimation can then be applied to WEC. Adjustments to the WEC for the existing wave frequency will allow for optimal performance and energy extraction.

## Bibliography

- [1] K. M. Bailey , P. C. Tay and H. B. Karayaka, "A Filterbank Method to Determine Ocean Wave Frequency," in *IEEE SSIAI*, 2016.
- [2] C. Göttlinger, "Maximally Decimated Filterbanks," 15 May 2007. [Online]. Available: <https://www2.spsc.tugraz.at/www-archive/AdvancedSignalProcessing/SS07-MultirateSystems/data/AdvancedSignalProcessing.pdf>. [Accessed 5 February 2016].
- [3] A. V. Oppenheim, A. S. Willsky and S. H. Nawab, *Signals & Systems*, Upper Saddle River, New Jersey: Prentice Hall , 1997, p. 518.
- [4] "Gonzalo Stirs Up Sediment and the Carbon Cycle," 26 October 2014. [Online]. Available: <http://earthobservatory.nasa.gov/IOTD/view.php?id=84595>. [Accessed 5 February 2016].
- [5] "Nishinoshima continues to erupt," 1 March 2105. [Online]. Available: <http://earthobservatory.nasa.gov/NaturalHazards/view.php?id=85449>. [Accessed 5 February 2016].
- [6] "Seeing the Reef for the Corals," 31 January 2016. [Online]. Available: <http://earthobservatory.nasa.gov/IOTD/view.php?id=87423>. [Accessed 5 February 2016].
- [7] "The Alphabet from Orbit: Letter J," 23 December 2015. [Online]. Available: <http://earthobservatory.nasa.gov/IOTD/view.php?id=87208>. [Accessed 5 February 2016].

## Appendices

## APPENDIX A: High Resolution Energy Tables

Table A. 1: Energy of Bermuda

$E_{l,k}$	0	1	2	3	4	5
0	0.000000	0.006329	0.004151	0.003343	0.002901	0.002490
1	0.007800	0.004871	0.003810	0.003558	0.003382	0.002945
2	0.004686	0.004051	0.003996	0.003935	0.003436	0.003078
3	0.003671	0.003463	0.003829	0.003785	0.003489	0.002997
4	0.003470	0.003374	0.003361	0.003278	0.003081	0.003029
5	0.004026	0.004139	0.003613	0.003174	0.003056	0.003114
6	0.006113	0.006448	0.004930	0.003859	0.003665	0.003787
7	0.011258	0.010016	0.006737	0.004598	0.004226	0.004307
8	0.015924	0.012305	0.008062	0.005500	0.004886	0.004862
9	0.015926	0.011819	0.007915	0.005816	0.004710	0.004330
10	0.012531	0.010349	0.007664	0.005817	0.004560	0.003654
11	0.009764	0.009271	0.007512	0.005712	0.004373	0.003791
12	0.007675	0.008147	0.006844	0.005579	0.004349	0.003623
13	0.006433	0.006416	0.005997	0.005002	0.004100	0.003483
14	0.005349	0.005424	0.005539	0.004758	0.003894	0.003333
15	0.004344	0.004505	0.004384	0.004194	0.003751	0.003095
16	0.004112	0.004173	0.003941	0.003812	0.003406	0.002999
17	0.003658	0.003777	0.003818	0.003447	0.003498	0.003313
18	0.003223	0.003152	0.003344	0.003396	0.003255	0.003013
19	0.002901	0.002762	0.003036	0.002930	0.002787	0.002718
20	0.002468	0.002498	0.002747	0.002748	0.002714	0.002478
21	0.002415	0.002430	0.002463	0.002415	0.002435	0.002244
22	0.002300	0.002241	0.002111	0.002142	0.001959	0.002061
23	0.002021	0.002015	0.001983	0.001899	0.001915	0.001840
24	0.001933	0.001905	0.001844	0.001710	0.001790	0.001723
25	0.001746	0.001837	0.001690	0.001745	0.001771	0.001714
26	0.001618	0.001655	0.001720	0.001636	0.001691	0.001545
27	0.001592	0.001595	0.001667	0.001678	0.001519	0.001565
28	0.001630	0.001554	0.001529	0.001515	0.001412	0.001449
29	0.001628	0.001538	0.001504	0.001525	0.001431	0.001485
30	0.001507	0.001465	0.001546	0.001526	0.001410	0.001473
31	0.001506	0.001486	0.001428	0.001434	0.001402	0.001406
32	0.001351	0.001451	0.001455	0.001407	0.001413	0.001404

Table A.1: Energy of Bermuda Cont'd

6	7	8	9	10	11
0.002243	0.002051	0.001996	0.001967	0.001919	0.001890
0.002579	0.002385	0.002416	0.002363	0.002161	0.002132
0.002807	0.002636	0.002568	0.002541	0.002491	0.002240
0.002902	0.002798	0.002711	0.002407	0.002533	0.002327
0.003097	0.002952	0.002894	0.002553	0.002605	0.002481
0.003469	0.003277	0.002964	0.002914	0.002716	0.002577
0.003754	0.003660	0.003092	0.002764	0.002682	0.002665
0.004449	0.003893	0.003418	0.003135	0.002803	0.002709
0.004841	0.004101	0.003334	0.003079	0.002737	0.002610
0.004272	0.003714	0.003043	0.002948	0.002782	0.002540
0.003643	0.003271	0.002950	0.002909	0.002848	0.002523
0.003685	0.003110	0.002984	0.002951	0.002812	0.002463
0.003411	0.003068	0.002724	0.002656	0.002483	0.002292
0.003105	0.002799	0.002705	0.002581	0.002182	0.002068
0.002983	0.002693	0.002555	0.002375	0.002079	0.001957
0.002777	0.002648	0.002516	0.002205	0.001992	0.001883
0.002699	0.002325	0.002311	0.002291	0.001964	0.001932
0.002810	0.002421	0.002232	0.002115	0.002027	0.001806
0.002573	0.002314	0.002154	0.001958	0.001916	0.001778
0.002486	0.002315	0.002033	0.001869	0.001795	0.001683
0.002302	0.002186	0.002113	0.001926	0.001797	0.001635
0.002163	0.002001	0.002002	0.001885	0.001648	0.001575
0.002019	0.001996	0.001752	0.001620	0.001568	0.001460
0.001804	0.001867	0.001647	0.001524	0.001405	0.001321
0.001521	0.001695	0.001606	0.001502	0.001418	0.001310
0.001574	0.001595	0.001508	0.001459	0.001335	0.001223
0.001589	0.001545	0.001403	0.001332	0.001305	0.001276
0.001593	0.001339	0.001201	0.001223	0.001201	0.001182
0.001389	0.001334	0.001303	0.001236	0.001169	0.001163
0.001424	0.001346	0.001329	0.001254	0.001256	0.001161
0.001447	0.001356	0.001264	0.001246	0.001229	0.001125
0.001429	0.001332	0.001241	0.001287	0.001224	0.001145
0.001379	0.001371	0.001457	0.001310	0.001237	0.001105

Table A.1: Energy of Bermuda Cont'd

12	13	14	15	16	17
0.001880	0.001751	0.001664	0.001394	0.001284	0.001128
0.002040	0.001838	0.001665	0.001424	0.001265	0.001267
0.002218	0.001840	0.001699	0.001591	0.001414	0.001323
0.002263	0.002109	0.001766	0.001600	0.001473	0.001399
0.002417	0.002265	0.001900	0.001656	0.001529	0.001445
0.002476	0.002258	0.001937	0.001685	0.001550	0.001451
0.002521	0.002253	0.001885	0.001768	0.001663	0.001426
0.002453	0.002241	0.001927	0.001750	0.001646	0.001468
0.002423	0.002219	0.001872	0.001750	0.001680	0.001475
0.002398	0.002066	0.001882	0.001732	0.001511	0.001313
0.002226	0.002014	0.001854	0.001756	0.001528	0.001399
0.002157	0.001884	0.001724	0.001621	0.001535	0.001417
0.002062	0.001983	0.001665	0.001533	0.001488	0.001392
0.001841	0.001845	0.001663	0.001535	0.001409	0.001419
0.002012	0.001789	0.001571	0.001564	0.001420	0.001306
0.001964	0.001771	0.001659	0.001505	0.001368	0.001278
0.001846	0.001696	0.001581	0.001410	0.001395	0.001274
0.001642	0.001615	0.001522	0.001348	0.001284	0.001286
0.001588	0.001551	0.001510	0.001386	0.001242	0.001152
0.001515	0.001518	0.001468	0.001403	0.001187	0.001127
0.001603	0.001382	0.001282	0.001271	0.001203	0.001134
0.001520	0.001360	0.001258	0.001210	0.001211	0.001143
0.001376	0.001345	0.001318	0.001213	0.001154	0.001096
0.001289	0.001340	0.001192	0.001161	0.001088	0.001045
0.001260	0.001167	0.001100	0.001044	0.000993	0.000928
0.001150	0.001090	0.001043	0.001037	0.001002	0.000932
0.001122	0.001146	0.001073	0.000967	0.000942	0.000935
0.001141	0.001101	0.001026	0.000972	0.000981	0.000880
0.001114	0.001067	0.000976	0.000982	0.000979	0.000939
0.001062	0.001047	0.000966	0.000936	0.000977	0.000970
0.001064	0.001010	0.000925	0.000941	0.000921	0.000897
0.001089	0.001033	0.001017	0.001012	0.000964	0.000923
0.001080	0.001117	0.001099	0.001027	0.000984	0.000964

Table A.1: Energy of Bermuda Cont'd

18	19	20	21	22	23
0.001081	0.001106	0.001061	0.001026	0.001027	0.000971
0.001223	0.001142	0.001096	0.001061	0.000999	0.000994
0.001238	0.001203	0.001160	0.001143	0.001092	0.000972
0.001349	0.001281	0.001231	0.001182	0.001049	0.000945
0.001476	0.001379	0.001293	0.001164	0.001053	0.000980
0.001404	0.001286	0.001204	0.001174	0.001090	0.000992
0.001419	0.001277	0.001160	0.001069	0.000988	0.000953
0.001333	0.001287	0.001246	0.001081	0.000936	0.000926
0.001393	0.001284	0.001187	0.001170	0.001021	0.000964
0.001333	0.001229	0.001147	0.001200	0.001065	0.000970
0.001236	0.001200	0.001113	0.001041	0.001011	0.000965
0.001222	0.001144	0.001115	0.001055	0.000974	0.000943
0.001245	0.001142	0.001112	0.001054	0.000980	0.000977
0.001206	0.001122	0.001141	0.001061	0.001000	0.000954
0.001197	0.001166	0.001148	0.001047	0.000896	0.000924
0.001200	0.001144	0.001120	0.001011	0.000914	0.000929
0.001218	0.001108	0.001041	0.000959	0.000914	0.000895
0.001277	0.001083	0.000962	0.000954	0.000960	0.000902
0.001128	0.001061	0.001007	0.000938	0.000928	0.000867
0.001080	0.001016	0.000978	0.000922	0.000931	0.000862
0.001032	0.001010	0.000920	0.000903	0.000904	0.000846
0.001025	0.000990	0.000925	0.000899	0.000874	0.000839
0.000983	0.000955	0.000991	0.000920	0.000817	0.000850
0.001000	0.001035	0.000923	0.000818	0.000796	0.000768
0.000991	0.000969	0.000891	0.000786	0.000815	0.000774
0.000980	0.000914	0.000916	0.000847	0.000836	0.000732
0.001039	0.000957	0.000890	0.000872	0.000791	0.000715
0.000952	0.000928	0.000874	0.000810	0.000746	0.000752
0.000877	0.000958	0.000905	0.000844	0.000755	0.000713
0.000870	0.000865	0.000828	0.000804	0.000780	0.000745
0.000871	0.000876	0.000831	0.000758	0.000785	0.000800
0.000893	0.000908	0.000889	0.000828	0.000760	0.000748
0.000958	0.000919	0.000921	0.000836	0.000780	0.000732

Table A.1: Energy of Bermuda Cont'd

24	25	26	27	28	29
0.000935	0.000947	0.000890	0.000876	0.000800	0.000833
0.000911	0.000893	0.000894	0.000837	0.000820	0.000835
0.000873	0.000905	0.000879	0.000858	0.000880	0.000861
0.000838	0.000928	0.000881	0.000863	0.000895	0.000900
0.001038	0.000989	0.000871	0.000861	0.000869	0.000912
0.001041	0.001012	0.000867	0.000891	0.000918	0.000904
0.000962	0.000959	0.000880	0.000971	0.000944	0.000906
0.000978	0.000926	0.000907	0.000999	0.000986	0.001132
0.000978	0.000952	0.000933	0.000876	0.000873	0.000905
0.000985	0.000892	0.000872	0.000917	0.000883	0.000884
0.001005	0.000871	0.000787	0.000855	0.000846	0.000839
0.000888	0.000828	0.000807	0.000850	0.000843	0.000814
0.000907	0.000826	0.000860	0.000859	0.000789	0.000777
0.000915	0.000840	0.000841	0.000783	0.000753	0.000775
0.000875	0.000807	0.000799	0.000761	0.000757	0.000768
0.000884	0.000837	0.000775	0.000758	0.000736	0.000765
0.000834	0.000822	0.000743	0.000750	0.000758	0.000759
0.000847	0.000829	0.000776	0.000738	0.000703	0.000681
0.000849	0.000803	0.000815	0.000718	0.000673	0.000676
0.000856	0.000801	0.000775	0.000718	0.000736	0.000718
0.000826	0.000772	0.000738	0.000698	0.000697	0.000709
0.000808	0.000782	0.000735	0.000713	0.000695	0.000719
0.000845	0.000737	0.000666	0.000657	0.000649	0.000695
0.000755	0.000742	0.000722	0.000695	0.000690	0.000677
0.000743	0.000684	0.000693	0.000643	0.000673	0.000695
0.000710	0.000691	0.000647	0.000634	0.000709	0.000662
0.000676	0.000693	0.000641	0.000696	0.000698	0.000619
0.000689	0.000684	0.000653	0.000692	0.000664	0.000601
0.000684	0.000658	0.000645	0.000643	0.000686	0.000621
0.000712	0.000674	0.000686	0.000693	0.000687	0.000607
0.000736	0.000668	0.000680	0.000655	0.000642	0.000623
0.000763	0.000717	0.000666	0.000651	0.000605	0.000644
0.000743	0.000704	0.000683	0.000663	0.000647	0.000610

Table A.1: Energy of Bermuda Cont'd

30	31	32
0.000800	0.000883	0.000860
0.000838	0.000826	0.000833
0.000862	0.000823	0.000833
0.000848	0.000782	0.000790
0.000782	0.000752	0.000789
0.000802	0.000789	0.000833
0.000851	0.000857	0.000796
0.001075	0.001004	0.000915
0.000926	0.000920	0.000948
0.000878	0.000860	0.000850
0.000783	0.000850	0.000854
0.000734	0.000832	0.000882
0.000795	0.000775	0.000777
0.000787	0.000800	0.000741
0.000787	0.000791	0.000732
0.000746	0.000763	0.000737
0.000743	0.000772	0.000770
0.000719	0.000694	0.000693
0.000670	0.000679	0.000691
0.000731	0.000729	0.000718
0.000735	0.000672	0.000669
0.000720	0.000672	0.000657
0.000675	0.000706	0.000692
0.000645	0.000686	0.000658
0.000623	0.000655	0.000662
0.000623	0.000628	0.000629
0.000589	0.000622	0.000621
0.000578	0.000609	0.000642
0.000580	0.000591	0.000600
0.000632	0.000553	0.000575
0.000614	0.000592	0.000607
0.000596	0.000589	0.000612
0.000594	0.000592	0.000590

Table A. 2: Energy of Nishinoshima

$E_{l,k}$	0	1	2	3	4	5
0	0.000000	0.010621	0.005238	0.004042	0.003719	0.003629
1	0.008713	0.006466	0.004393	0.003842	0.004163	0.004642
2	0.004728	0.004069	0.003771	0.003467	0.003694	0.005201
3	0.003975	0.003822	0.003853	0.004137	0.004680	0.006225
4	0.004156	0.004041	0.004455	0.005150	0.006901	0.008761
5	0.005870	0.005675	0.007202	0.007607	0.008727	0.010542
6	0.008786	0.009198	0.010851	0.011560	0.012349	0.012749
7	0.011476	0.012859	0.013996	0.014523	0.014136	0.012726
8	0.012856	0.014904	0.014902	0.014294	0.013328	0.011502
9	0.011622	0.013238	0.012399	0.011515	0.010894	0.010254
10	0.009478	0.010267	0.010136	0.010084	0.009079	0.008618
11	0.007992	0.008534	0.008771	0.008683	0.007949	0.007746
12	0.007475	0.007658	0.007673	0.007148	0.007190	0.007349
13	0.006745	0.007104	0.007212	0.006507	0.006557	0.006770
14	0.006112	0.006397	0.006303	0.006263	0.006273	0.006494
15	0.005603	0.005806	0.005672	0.005380	0.005456	0.005748
16	0.005096	0.005395	0.005121	0.005143	0.005214	0.005458
17	0.004452	0.004549	0.004329	0.004687	0.004671	0.004497
18	0.004316	0.004327	0.003983	0.004231	0.004292	0.004194
19	0.004031	0.003714	0.004031	0.004023	0.003972	0.004169
20	0.003769	0.003786	0.003917	0.004007	0.003956	0.003719
21	0.003506	0.003719	0.003615	0.003623	0.003705	0.003337
22	0.003201	0.003287	0.003278	0.003416	0.003213	0.003180
23	0.002672	0.002787	0.002890	0.003068	0.002882	0.003064
24	0.002560	0.002654	0.002902	0.002799	0.002683	0.002606
25	0.002417	0.002443	0.002519	0.002637	0.002666	0.002548
26	0.002308	0.002294	0.002393	0.002398	0.002328	0.002375
27	0.002146	0.002262	0.002303	0.002287	0.002388	0.002403
28	0.001963	0.002130	0.002114	0.002143	0.002211	0.002295
29	0.001990	0.001931	0.002007	0.002040	0.001885	0.002000
30	0.001889	0.001896	0.002002	0.001985	0.001861	0.001829
31	0.001924	0.001789	0.001844	0.001864	0.001705	0.001763
32	0.001698	0.001802	0.001873	0.001872	0.001698	0.001647

Table A. 2: Energy of Nishinoshima Cont'd

6	7	8	9	10	11
0.003874	0.003971	0.003636	0.003583	0.003506	0.003090
0.005444	0.006593	0.005630	0.004258	0.003556	0.003162
0.007383	0.010274	0.009684	0.006667	0.005242	0.004438
0.008542	0.011190	0.010386	0.008169	0.006144	0.005524
0.010083	0.010468	0.008788	0.007188	0.006232	0.005548
0.011086	0.010043	0.008082	0.006886	0.006181	0.005753
0.011507	0.010332	0.008627	0.007035	0.006146	0.005550
0.010988	0.009534	0.008019	0.006575	0.006102	0.005402
0.010919	0.009083	0.007430	0.006708	0.005707	0.004997
0.009859	0.007949	0.006988	0.006166	0.005321	0.004699
0.008000	0.006932	0.006863	0.005996	0.005019	0.004874
0.006795	0.006875	0.006606	0.005994	0.005034	0.004789
0.006948	0.006655	0.006110	0.005495	0.005087	0.004613
0.006849	0.006015	0.005500	0.005440	0.004970	0.004539
0.006263	0.005739	0.005233	0.005155	0.004349	0.004357
0.005790	0.005310	0.004985	0.004718	0.004169	0.003803
0.005199	0.004978	0.004815	0.004288	0.004151	0.003782
0.004377	0.004557	0.004602	0.004141	0.004015	0.003880
0.003916	0.004110	0.004198	0.003680	0.003649	0.003556
0.004248	0.003940	0.003693	0.003585	0.003861	0.003407
0.003811	0.003710	0.003719	0.003357	0.003255	0.003096
0.003358	0.003538	0.003501	0.003032	0.002953	0.002938
0.003059	0.003393	0.003116	0.003099	0.002905	0.002790
0.002935	0.003094	0.002897	0.002718	0.002742	0.002530
0.002794	0.002848	0.002723	0.002625	0.002527	0.002310
0.002576	0.002540	0.002525	0.002658	0.002503	0.002459
0.002442	0.002465	0.002379	0.002425	0.002398	0.002251
0.002141	0.002195	0.002235	0.002228	0.002051	0.002128
0.002100	0.002047	0.002106	0.002123	0.001998	0.002115
0.001882	0.001898	0.002110	0.001928	0.001902	0.001902
0.001755	0.001774	0.001802	0.001803	0.001704	0.001767
0.001734	0.001987	0.001880	0.001670	0.001615	0.001615
0.001905	0.004230	0.002542	0.001565	0.001577	0.001575

Table A. 2: Energy of Nishinoshima Cont'd

12	13	14	15	16	17
0.002929	0.002730	0.002455	0.002134	0.001962	0.001924
0.003106	0.002816	0.002482	0.002230	0.002117	0.002026
0.003769	0.003171	0.002978	0.002454	0.002295	0.002301
0.004686	0.004073	0.003498	0.003210	0.002686	0.002558
0.004970	0.004532	0.003925	0.003546	0.003134	0.002888
0.004744	0.004164	0.003874	0.003534	0.003270	0.003074
0.004744	0.003984	0.003711	0.003422	0.003279	0.003149
0.004547	0.004226	0.003787	0.003568	0.003163	0.002989
0.004319	0.003861	0.003735	0.003501	0.003005	0.002677
0.004431	0.003968	0.003577	0.003185	0.002840	0.002773
0.004243	0.003952	0.003575	0.003264	0.003008	0.002823
0.004390	0.003817	0.003654	0.003288	0.003116	0.002750
0.004049	0.003741	0.003303	0.003185	0.003044	0.002622
0.004129	0.003694	0.003350	0.003095	0.002912	0.002763
0.003641	0.003643	0.003401	0.002901	0.002924	0.002810
0.003605	0.003172	0.003148	0.002961	0.002861	0.002631
0.003451	0.002835	0.002977	0.002879	0.002610	0.002541
0.003283	0.002975	0.002875	0.002689	0.002718	0.002558
0.003251	0.002962	0.002885	0.002626	0.002624	0.002396
0.002934	0.002731	0.002835	0.002697	0.002488	0.002293
0.003030	0.002741	0.002578	0.002482	0.002342	0.002194
0.002917	0.002690	0.002584	0.002393	0.002018	0.002017
0.002624	0.002492	0.002192	0.002161	0.001862	0.001880
0.002355	0.002277	0.002163	0.002081	0.001873	0.001837
0.002398	0.002237	0.002269	0.001956	0.001944	0.001979
0.002258	0.002073	0.002036	0.001871	0.001881	0.001816
0.002123	0.002001	0.001955	0.001826	0.001817	0.001739
0.002123	0.001820	0.001854	0.001780	0.001689	0.001622
0.002055	0.001807	0.001686	0.001639	0.001636	0.001603
0.001887	0.001770	0.001601	0.001527	0.001716	0.001650
0.001689	0.001653	0.001659	0.001526	0.001465	0.001481
0.001456	0.001466	0.001486	0.001478	0.001419	0.001435
0.001556	0.001424	0.001465	0.001450	0.001373	0.001398

Table A. 2: Energy of Nishinoshima Cont'd

18	19	20	21	22	23
0.001796	0.001748	0.001704	0.001659	0.001592	0.001561
0.001841	0.001877	0.001752	0.001681	0.001623	0.001599
0.001907	0.001869	0.001892	0.001711	0.001695	0.001608
0.002275	0.002122	0.001991	0.001783	0.001763	0.001608
0.002699	0.002502	0.002323	0.002090	0.002010	0.001712
0.002742	0.002654	0.002367	0.002148	0.002149	0.001882
0.002899	0.002765	0.002617	0.002424	0.002156	0.001949
0.002721	0.002659	0.002570	0.002274	0.001991	0.001921
0.002700	0.002557	0.002429	0.002321	0.002060	0.001935
0.002625	0.002632	0.002592	0.002392	0.002146	0.001882
0.002499	0.002457	0.002421	0.002280	0.002124	0.001918
0.002423	0.002396	0.002311	0.002183	0.002150	0.001843
0.002334	0.002399	0.002168	0.001973	0.001959	0.001795
0.002329	0.002237	0.002055	0.001872	0.001765	0.001797
0.002466	0.002297	0.002031	0.001853	0.001805	0.001808
0.002486	0.002247	0.001876	0.001833	0.001782	0.001840
0.002491	0.002171	0.001845	0.002006	0.001711	0.001704
0.002173	0.002207	0.001988	0.001862	0.001661	0.001584
0.002125	0.001958	0.001880	0.001753	0.001599	0.001530
0.002069	0.002035	0.001813	0.001688	0.001572	0.001534
0.002045	0.001957	0.001824	0.001808	0.001516	0.001480
0.001939	0.001818	0.001700	0.001661	0.001544	0.001454
0.001906	0.001686	0.001661	0.001525	0.001466	0.001417
0.001774	0.001619	0.001623	0.001436	0.001442	0.001402
0.001668	0.001553	0.001598	0.001477	0.001436	0.001338
0.001674	0.001496	0.001461	0.001381	0.001364	0.001275
0.001612	0.001416	0.001379	0.001278	0.001285	0.001251
0.001545	0.001479	0.001446	0.001228	0.001199	0.001195
0.001447	0.001297	0.001276	0.001256	0.001124	0.001184
0.001517	0.001356	0.001288	0.001194	0.001109	0.001169
0.001471	0.001409	0.001324	0.001221	0.001169	0.001162
0.001449	0.001353	0.001234	0.001179	0.001099	0.001081
0.001323	0.001231	0.001135	0.001240	0.001090	0.001099

Table A. 2: Energy of Nishinoshima Cont'd

24	25	26	27	28	29
0.001536	0.001509	0.001473	0.001503	0.001449	0.001454
0.001512	0.001526	0.001515	0.001519	0.001484	0.001530
0.001564	0.001522	0.001563	0.001516	0.001509	0.001501
0.001569	0.001644	0.001603	0.001524	0.001553	0.001556
0.001666	0.001637	0.001652	0.001612	0.001509	0.001558
0.001806	0.001844	0.001654	0.001668	0.001628	0.001558
0.001721	0.001713	0.001618	0.001580	0.001534	0.001571
0.001772	0.001783	0.001644	0.001551	0.001456	0.001453
0.001888	0.001884	0.001624	0.001485	0.001590	0.001475
0.001834	0.001674	0.001635	0.001636	0.001661	0.001549
0.001791	0.001711	0.001709	0.001698	0.001705	0.001547
0.001855	0.001661	0.001603	0.001748	0.001543	0.001447
0.001768	0.001569	0.001547	0.001608	0.001496	0.001442
0.001596	0.001629	0.001652	0.001616	0.001492	0.001419
0.001580	0.001644	0.001573	0.001473	0.001458	0.001376
0.001616	0.001408	0.001493	0.001348	0.001376	0.001279
0.001546	0.001447	0.001490	0.001398	0.001239	0.001215
0.001495	0.001372	0.001397	0.001360	0.001266	0.001180
0.001414	0.001341	0.001383	0.001396	0.001187	0.001159
0.001419	0.001313	0.001370	0.001322	0.001210	0.001147
0.001391	0.001324	0.001281	0.001289	0.001220	0.001226
0.001365	0.001291	0.001196	0.001173	0.001088	0.001096
0.001274	0.001250	0.001127	0.001135	0.001039	0.001040
0.001241	0.001189	0.001044	0.001174	0.001130	0.001037
0.001217	0.001234	0.001136	0.001081	0.000999	0.001037
0.001255	0.001213	0.001103	0.001040	0.001019	0.001067
0.001228	0.001173	0.001089	0.000994	0.000991	0.001002
0.001223	0.001089	0.001031	0.000984	0.001046	0.000992
0.001184	0.001074	0.001074	0.001083	0.001095	0.000981
0.001200	0.001123	0.001026	0.001055	0.001013	0.000966
0.001170	0.001038	0.000941	0.000935	0.000957	0.000915
0.001055	0.001052	0.000977	0.001001	0.001010	0.000942
0.001103	0.001041	0.000971	0.001021	0.001036	0.000968

Table A. 2: Energy of Nishinoshima Cont'd

30	31	32
0.001448	0.001460	0.001429
0.001496	0.001497	0.001484
0.001462	0.001466	0.001490
0.001486	0.001421	0.001500
0.001534	0.001485	0.001564
0.001498	0.001475	0.001544
0.001597	0.001613	0.001589
0.001562	0.001742	0.001842
0.001489	0.001428	0.001408
0.001393	0.001382	0.001396
0.001568	0.001468	0.001387
0.001491	0.001362	0.001277
0.001353	0.001293	0.001268
0.001431	0.001331	0.001332
0.001332	0.001337	0.001311
0.001260	0.001222	0.001205
0.001171	0.001213	0.001155
0.001214	0.001207	0.001144
0.001229	0.001241	0.001159
0.001114	0.001136	0.001061
0.001127	0.001063	0.001039
0.001082	0.001019	0.000972
0.001051	0.001019	0.000944
0.000981	0.000974	0.001007
0.000969	0.000930	0.000930
0.000948	0.000958	0.000937
0.000964	0.000916	0.000911
0.000902	0.000953	0.000878
0.000840	0.000843	0.000837
0.000835	0.000855	0.000874
0.000927	0.000885	0.000854
0.000908	0.000928	0.000866
0.000884	0.000893	0.000819

Table A. 3: Energy of Palau

$E_{l,k}$	0	1	2	3	4	5
0	0.000000	<b>0.015949</b>	0.010260	0.007064	0.006712	0.007979
1	0.014344	0.010053	0.006967	0.005747	0.005957	0.006979
2	0.008337	0.007085	0.005187	0.004636	0.004478	0.004206
3	0.006414	0.005260	0.004180	0.003916	0.003859	0.003537
4	0.004773	0.004000	0.003564	0.003335	0.003203	0.003174
5	0.003251	0.002985	0.002906	0.002904	0.002708	0.002484
6	0.002538	0.002519	0.002422	0.002657	0.002559	0.002427
7	0.002030	0.002010	0.002004	0.002236	0.002088	0.002103
8	0.001908	0.001899	0.001977	0.002021	0.001850	0.001814
9	0.001733	0.001669	0.001612	0.001640	0.001680	0.001645
10	0.001586	0.001475	0.001500	0.001513	0.001578	0.001480
11	0.001425	0.001360	0.001403	0.001331	0.001474	0.001509
12	0.001491	0.001328	0.001197	0.001207	0.001324	0.001380
13	0.001320	0.001240	0.001174	0.001188	0.001223	0.001256
14	0.001173	0.001126	0.001062	0.001085	0.001187	0.001126
15	0.001130	0.001050	0.001024	0.001090	0.001133	0.001150
16	0.001082	0.001000	0.001010	0.001017	0.001045	0.001079
17	0.001090	0.001006	0.000955	0.000963	0.000990	0.001017
18	0.001050	0.000969	0.000920	0.000987	0.001027	0.001007
19	0.000966	0.000959	0.000904	0.001033	0.001007	0.000986
20	0.000917	0.000975	0.000884	0.000871	0.000895	0.000949
21	0.000919	0.000847	0.000891	0.000887	0.000850	0.000895
22	0.000867	0.000825	0.000818	0.000843	0.000813	0.000888
23	0.000821	0.000854	0.000776	0.000786	0.000761	0.000844
24	0.000888	0.000807	0.000848	0.000790	0.000774	0.000834
25	0.000820	0.000787	0.000743	0.000747	0.000703	0.000757
26	0.000768	0.000751	0.000755	0.000770	0.000741	0.000737
27	0.000735	0.000661	0.000711	0.000759	0.000752	0.000740
28	0.000725	0.000697	0.000714	0.000702	0.000713	0.000708
29	0.000711	0.000704	0.000731	0.000697	0.000679	0.000731
30	0.000745	0.000688	0.000699	0.000721	0.000654	0.000686
31	0.000691	0.000628	0.000672	0.000700	0.000712	0.000705
32	0.000710	0.000618	0.000657	0.000701	0.000706	0.000715

Table A. 3: Energy of Palau Cont'd

6	7	8	9	10	11
0.007525	0.006500	0.005296	0.004500	0.004202	0.003769
0.007083	0.006105	0.005334	0.004918	0.004480	0.003862
0.004173	0.003705	0.003599	0.003504	0.003192	0.003041
0.003263	0.003121	0.002812	0.002616	0.002335	0.002306
0.003096	0.002762	0.002525	0.002239	0.002104	0.001912
0.002641	0.002320	0.002233	0.002060	0.002029	0.001850
0.002108	0.002051	0.002176	0.001997	0.002017	0.001794
0.001966	0.001825	0.001922	0.001873	0.001850	0.001780
0.001814	0.001854	0.001809	0.001831	0.001799	0.001721
0.001641	0.001771	0.001723	0.001678	0.001744	0.001692
0.001515	0.001469	0.001519	0.001578	0.001694	0.001572
0.001526	0.001413	0.001379	0.001391	0.001543	0.001575
0.001303	0.001258	0.001239	0.001194	0.001294	0.001398
0.001225	0.001152	0.001245	0.001178	0.001204	0.001272
0.001210	0.001234	0.001175	0.001150	0.001236	0.001305
0.001178	0.001089	0.001121	0.001158	0.001185	0.001154
0.001123	0.001164	0.001158	0.001125	0.001134	0.001043
0.001048	0.001090	0.001011	0.001043	0.001056	0.001066
0.001035	0.001074	0.001035	0.001071	0.001082	0.001031
0.000974	0.000978	0.001008	0.001050	0.001020	0.000977
0.001006	0.001013	0.000997	0.000993	0.000928	0.000896
0.000978	0.001016	0.000957	0.000923	0.001011	0.001012
0.000893	0.000956	0.000925	0.000954	0.000974	0.000932
0.000856	0.000891	0.000887	0.000935	0.000898	0.000913
0.000919	0.000889	0.000851	0.000871	0.000899	0.000880
0.000811	0.000824	0.000814	0.000815	0.000838	0.000856
0.000756	0.000799	0.000761	0.000777	0.000752	0.000822
0.000735	0.000769	0.000744	0.000724	0.000724	0.000732
0.000692	0.000726	0.000714	0.000736	0.000755	0.000698
0.000735	0.000756	0.000763	0.000749	0.000751	0.000696
0.000691	0.000702	0.000708	0.000690	0.000678	0.000712
0.000820	0.000775	0.000677	0.000707	0.000690	0.000667
0.001352	0.001272	0.000682	0.000693	0.000655	0.000649

Table A. 3: Energy of Palau Cont'd

12	13	14	15	16	17
0.003463	0.003097	0.002839	0.002580	0.002395	0.002298
0.003295	0.003296	0.002794	0.002508	0.002483	0.002196
0.002846	0.002774	0.002492	0.002376	0.002263	0.001986
0.002412	0.002328	0.002380	0.002186	0.001957	0.001968
0.002088	0.002080	0.002080	0.001905	0.001822	0.001813
0.001753	0.001740	0.001775	0.001697	0.001626	0.001584
0.001756	0.001726	0.001472	0.001526	0.001465	0.001383
0.001626	0.001708	0.001635	0.001523	0.001356	0.001312
0.001606	0.001668	0.001622	0.001545	0.001408	0.001208
0.001673	0.001541	0.001589	0.001486	0.001359	0.001165
0.001535	0.001494	0.001466	0.001428	0.001332	0.001275
0.001555	0.001484	0.001445	0.001378	0.001258	0.001207
0.001412	0.001367	0.001213	0.001208	0.001192	0.001206
0.001347	0.001339	0.001194	0.001209	0.001247	0.001177
0.001200	0.001212	0.001164	0.001115	0.001216	0.001204
0.001149	0.001150	0.001123	0.001148	0.001154	0.001085
0.001153	0.001071	0.001052	0.001032	0.001036	0.001022
0.001031	0.001021	0.000981	0.000995	0.001079	0.001066
0.000958	0.000958	0.000979	0.001027	0.001015	0.000932
0.000948	0.000903	0.000968	0.000889	0.000909	0.000929
0.000882	0.000874	0.000941	0.000882	0.000846	0.000871
0.000900	0.000880	0.000868	0.000821	0.000808	0.000849
0.000907	0.000836	0.000849	0.000791	0.000833	0.000868
0.000887	0.000818	0.000820	0.000809	0.000766	0.000810
0.000817	0.000787	0.000787	0.000806	0.000778	0.000766
0.000848	0.000786	0.000785	0.000746	0.000783	0.000755
0.000800	0.000767	0.000803	0.000734	0.000726	0.000685
0.000745	0.000705	0.000777	0.000697	0.000679	0.000713
0.000707	0.000739	0.000739	0.000648	0.000680	0.000676
0.000709	0.000711	0.000658	0.000676	0.000687	0.000609
0.000761	0.000671	0.000658	0.000722	0.000630	0.000622
0.000692	0.000692	0.000681	0.000659	0.000635	0.000686
0.000665	0.000696	0.000657	0.000628	0.000640	0.000639

Table A. 3: Energy of Palau Cont'd

18	19	20	21	22	23
0.002019	0.001881	0.001756	0.001857	0.001606	0.001463
0.001900	0.001828	0.001695	0.001651	0.001473	0.001461
0.001749	0.001800	0.001639	0.001465	0.001419	0.001379
0.001742	0.001694	0.001472	0.001350	0.001422	0.001350
0.001623	0.001639	0.001367	0.001360	0.001422	0.001351
0.001481	0.001459	0.001323	0.001367	0.001373	0.001355
0.001363	0.001391	0.001306	0.001294	0.001242	0.001222
0.001350	0.001307	0.001189	0.001122	0.001058	0.001138
0.001183	0.001170	0.001097	0.001107	0.001067	0.001120
0.001180	0.001256	0.001153	0.001063	0.001016	0.001026
0.001199	0.001156	0.001070	0.001032	0.001026	0.001032
0.001151	0.001157	0.001012	0.000965	0.001010	0.001019
0.001176	0.001060	0.000988	0.000999	0.000974	0.001000
0.001148	0.001049	0.001076	0.001039	0.000973	0.000961
0.001100	0.001107	0.001024	0.000977	0.000929	0.000897
0.001085	0.001060	0.001036	0.001014	0.000921	0.000939
0.000934	0.000993	0.001060	0.000982	0.000882	0.000946
0.000988	0.000930	0.000968	0.000919	0.000903	0.000976
0.000892	0.000908	0.000959	0.000889	0.000920	0.000870
0.000882	0.000898	0.000981	0.000926	0.000889	0.000814
0.000904	0.000844	0.000870	0.000894	0.000860	0.000844
0.000819	0.000797	0.000832	0.000846	0.000772	0.000847
0.000861	0.000825	0.000781	0.000811	0.000790	0.000757
0.000748	0.000827	0.000843	0.000794	0.000809	0.000747
0.000786	0.000824	0.000809	0.000804	0.000778	0.000755
0.000757	0.000725	0.000726	0.000782	0.000730	0.000714
0.000727	0.000724	0.000680	0.000707	0.000738	0.000711
0.000684	0.000638	0.000643	0.000681	0.000687	0.000672
0.000678	0.000643	0.000687	0.000691	0.000682	0.000643
0.000641	0.000632	0.000671	0.000671	0.000660	0.000629
0.000619	0.000609	0.000632	0.000664	0.000584	0.000632
0.000647	0.000634	0.000635	0.000610	0.000575	0.000615
0.000635	0.000639	0.000655	0.000590	0.000578	0.000614

Table A. 3: Energy of Palau Cont'd

24	25	26	27	28	29
0.001386	0.001428	0.001304	0.001271	0.001179	0.001112
0.001347	0.001258	0.001206	0.001173	0.001067	0.001032
0.001255	0.001203	0.001171	0.001144	0.001009	0.001030
0.001195	0.001114	0.001120	0.001053	0.001005	0.001060
0.001208	0.001074	0.001130	0.001005	0.001010	0.000999
0.001255	0.001073	0.001140	0.001149	0.001123	0.001062
0.001120	0.001027	0.001027	0.001080	0.001098	0.001133
0.001085	0.000976	0.000943	0.000933	0.000902	0.000954
0.001006	0.000979	0.000957	0.000965	0.000933	0.000951
0.000922	0.000922	0.000895	0.000918	0.000959	0.000981
0.000988	0.000935	0.000890	0.000885	0.000900	0.000858
0.000907	0.000917	0.000891	0.000898	0.000950	0.000897
0.000895	0.000836	0.000872	0.000900	0.000928	0.000885
0.000929	0.000830	0.000846	0.000835	0.000839	0.000846
0.000945	0.000854	0.000888	0.000951	0.000903	0.000856
0.000877	0.000863	0.000946	0.000900	0.000869	0.000802
0.000894	0.000862	0.000953	0.000921	0.000830	0.000789
0.000905	0.000823	0.000859	0.000874	0.000844	0.000755
0.000807	0.000805	0.000809	0.000813	0.000787	0.000752
0.000867	0.000804	0.000814	0.000788	0.000820	0.000782
0.000803	0.000786	0.000776	0.000830	0.000805	0.000742
0.000798	0.000855	0.000793	0.000775	0.000740	0.000742
0.000771	0.000774	0.000775	0.000747	0.000725	0.000722
0.000735	0.000714	0.000704	0.000685	0.000653	0.000679
0.000704	0.000694	0.000676	0.000669	0.000718	0.000697
0.000717	0.000716	0.000660	0.000661	0.000675	0.000709
0.000697	0.000684	0.000638	0.000657	0.000680	0.000700
0.000672	0.000656	0.000673	0.000640	0.000615	0.000652
0.000625	0.000619	0.000607	0.000620	0.000631	0.000655
0.000628	0.000594	0.000618	0.000608	0.000661	0.000692
0.000610	0.000624	0.000652	0.000615	0.000605	0.000668
0.000618	0.000562	0.000588	0.000603	0.000587	0.000609
0.000634	0.000633	0.000596	0.000570	0.000613	0.000592

Table A. 3: Energy of Palau Cont'd

30	31	32
0.001058	0.001093	0.001059
0.001013	0.001037	0.001020
0.001030	0.000989	0.000987
0.001046	0.000981	0.000974
0.000925	0.000904	0.000931
0.000928	0.000989	0.001013
0.001013	0.001016	0.001014
0.000903	0.000956	0.001025
0.000950	0.000953	0.000959
0.000993	0.000883	0.000980
0.000935	0.000896	0.000927
0.000930	0.000873	0.000909
0.000847	0.000863	0.000925
0.000851	0.000900	0.000923
0.000866	0.000844	0.000899
0.000862	0.000873	0.000893
0.000790	0.000786	0.000778
0.000784	0.000836	0.000826
0.000803	0.000772	0.000779
0.000773	0.000737	0.000770
0.000701	0.000761	0.000780
0.000750	0.000768	0.000787
0.000754	0.000778	0.000734
0.000714	0.000701	0.000708
0.000652	0.000703	0.000721
0.000670	0.000611	0.000672
0.000658	0.000648	0.000612
0.000646	0.000626	0.000605
0.000599	0.000584	0.000573
0.000644	0.000621	0.000601
0.000621	0.000650	0.000583
0.000604	0.000605	0.000626
0.000598	0.000595	0.000602

Table A. 4: Energy of Townsville

$E_{l,k}$	0	1	2	3	4	5
0	0.000000	0.027321	0.016755	0.014807	0.014435	0.011694
1	0.020946	0.014945	0.013165	0.011121	0.010312	0.009686
2	0.015298	0.012777	0.012092	0.010133	0.009197	0.008827
3	0.014857	0.011347	0.010389	0.009576	0.008894	0.008188
4	0.013387	0.011431	0.010159	0.009887	0.009091	0.008000
5	0.010452	0.009533	0.009265	0.008745	0.008210	0.007269
6	0.009386	0.008570	0.009049	0.008070	0.007295	0.006890
7	0.008615	0.007867	0.008142	0.007160	0.007461	0.006606
8	0.008131	0.007369	0.007170	0.007017	0.006736	0.005998
9	0.006885	0.006440	0.006285	0.005727	0.005569	0.005508
10	0.005683	0.005351	0.005118	0.005057	0.004810	0.004470
11	0.004815	0.004403	0.004268	0.004097	0.004021	0.003801
12	0.004168	0.003882	0.003837	0.003570	0.003614	0.003450
13	0.003308	0.003022	0.002878	0.002988	0.003032	0.002802
14	0.002697	0.002584	0.002684	0.002670	0.002603	0.002453
15	0.002374	0.002165	0.002179	0.002089	0.002014	0.001903
16	0.002196	0.001935	0.001835	0.001867	0.001739	0.001768
17	0.001930	0.001739	0.001662	0.001619	0.001572	0.001560
18	0.001750	0.001539	0.001493	0.001505	0.001479	0.001352
19	0.001472	0.001478	0.001351	0.001452	0.001329	0.001294
20	0.001435	0.001307	0.001197	0.001145	0.001142	0.001067
21	0.001299	0.001177	0.001141	0.001154	0.001025	0.000972
22	0.001147	0.000974	0.001002	0.001020	0.000968	0.000850
23	0.001100	0.000849	0.000862	0.000860	0.000816	0.000747
24	0.000935	0.000729	0.000749	0.000709	0.000699	0.000624
25	0.000748	0.000613	0.000599	0.000577	0.000535	0.000521
26	0.000649	0.000537	0.000510	0.000500	0.000432	0.000438
27	0.000679	0.000485	0.000456	0.000435	0.000420	0.000431
28	0.000621	0.000472	0.000434	0.000419	0.000419	0.000413
29	0.000847	0.000478	0.000428	0.000414	0.000406	0.000381
30	0.000861	0.000477	0.000437	0.000402	0.000399	0.000393
31	0.000591	0.000422	0.000424	0.000423	0.000426	0.000425
32	0.000600	0.000429	0.000387	0.000407	0.000423	0.000396

Table A. 4: Energy of Townsville Cont'd

6	7	8	9	10	11
0.010165	0.008612	0.008083	0.007295	0.006426	0.005871
0.008716	0.007466	0.006851	0.006340	0.005652	0.005276
0.007987	0.007386	0.006521	0.006200	0.005660	0.004593
0.007501	0.007504	0.006209	0.005665	0.005020	0.004344
0.007261	0.006627	0.006125	0.005929	0.005110	0.004446
0.006450	0.006151	0.006067	0.005327	0.004618	0.004327
0.006403	0.005858	0.005432	0.005208	0.004675	0.004209
0.005891	0.005295	0.005132	0.004485	0.004288	0.004059
0.005588	0.005159	0.004719	0.003965	0.003969	0.003908
0.005032	0.004680	0.004032	0.003743	0.003685	0.003411
0.004422	0.004058	0.003628	0.003224	0.003270	0.002974
0.003410	0.003471	0.003206	0.002910	0.002659	0.002429
0.003044	0.002944	0.002734	0.002415	0.002162	0.002028
0.002694	0.002625	0.002258	0.001962	0.001801	0.001739
0.002280	0.002259	0.001869	0.001743	0.001636	0.001504
0.001879	0.001830	0.001685	0.001542	0.001504	0.001205
0.001765	0.001705	0.001428	0.001305	0.001324	0.001103
0.001447	0.001406	0.001313	0.001199	0.001084	0.000983
0.001192	0.001219	0.001140	0.001029	0.000929	0.000859
0.001229	0.001146	0.000977	0.000897	0.000833	0.000829
0.000987	0.000937	0.000875	0.000869	0.000787	0.000761
0.000923	0.000824	0.000754	0.000740	0.000691	0.000647
0.000833	0.000749	0.000726	0.000693	0.000612	0.000572
0.000684	0.000666	0.000660	0.000573	0.000548	0.000537
0.000592	0.000586	0.000582	0.000515	0.000473	0.000457
0.000519	0.000480	0.000483	0.000452	0.000413	0.000395
0.000426	0.000421	0.000436	0.000439	0.000417	0.000405
0.000425	0.000435	0.000452	0.000421	0.000410	0.000396
0.000387	0.000381	0.000393	0.000384	0.000374	0.000362
0.000391	0.000408	0.000376	0.000356	0.000361	0.000365
0.000408	0.000372	0.000373	0.000375	0.000346	0.000346
0.000378	0.000375	0.000386	0.000355	0.000335	0.000346
0.000380	0.000369	0.000386	0.000386	0.000366	0.000378

Table A. 4: Energy of Townsville Cont'd

12	13	14	15	16	17
0.004924	0.004158	0.003794	0.003129	0.002877	0.002507
0.004384	0.003590	0.003045	0.002968	0.002670	0.002208
0.004150	0.003491	0.002948	0.002655	0.002415	0.002012
0.004071	0.003376	0.003008	0.002725	0.002384	0.002091
0.003959	0.003413	0.002759	0.002539	0.002292	0.001930
0.003929	0.003328	0.002799	0.002477	0.002199	0.001903
0.003730	0.003129	0.002661	0.002393	0.002144	0.001898
0.003512	0.003035	0.002468	0.002246	0.001998	0.001681
0.003496	0.002973	0.002337	0.002112	0.001737	0.001618
0.002852	0.002605	0.002168	0.001913	0.001633	0.001388
0.002466	0.002352	0.001924	0.001660	0.001499	0.001210
0.002254	0.002091	0.001827	0.001491	0.001282	0.001139
0.001925	0.001747	0.001486	0.001253	0.001068	0.000971
0.001699	0.001462	0.001166	0.001060	0.000952	0.000879
0.001372	0.001176	0.000976	0.000960	0.000857	0.000743
0.001127	0.001083	0.000880	0.000832	0.000806	0.000675
0.000980	0.000923	0.000824	0.000755	0.000622	0.000612
0.000914	0.000843	0.000722	0.000669	0.000649	0.000566
0.000801	0.000759	0.000693	0.000568	0.000581	0.000563
0.000752	0.000677	0.000676	0.000562	0.000496	0.000481
0.000640	0.000603	0.000562	0.000511	0.000455	0.000444
0.000613	0.000582	0.000492	0.000473	0.000449	0.000413
0.000521	0.000511	0.000465	0.000463	0.000428	0.000417
0.000489	0.000458	0.000413	0.000419	0.000394	0.000388
0.000423	0.000429	0.000408	0.000411	0.000396	0.000356
0.000388	0.000374	0.000367	0.000364	0.000378	0.000362
0.000370	0.000373	0.000369	0.000366	0.000342	0.000353
0.000370	0.000366	0.000353	0.000330	0.000352	0.000372
0.000381	0.000344	0.000358	0.000347	0.000355	0.000358
0.000354	0.000344	0.000353	0.000371	0.000356	0.000367
0.000339	0.000376	0.000375	0.000373	0.000349	0.000362
0.000371	0.000410	0.000363	0.000373	0.000380	0.000347
0.000357	0.000385	0.000349	0.000351	0.000375	0.000347

Table A. 4: Energy of Townsville Cont'd

18	19	20	21	22	23
0.002430	0.001911	0.001765	0.001563	0.001345	0.001239
0.001858	0.001679	0.001461	0.001319	0.001108	0.000924
0.001862	0.001626	0.001420	0.001343	0.001120	0.000911
0.001909	0.001662	0.001452	0.001264	0.001031	0.000846
0.001676	0.001550	0.001432	0.001251	0.001064	0.000804
0.001580	0.001460	0.001350	0.001163	0.000951	0.000757
0.001529	0.001380	0.001218	0.001079	0.000908	0.000731
0.001428	0.001325	0.001099	0.000943	0.000837	0.000695
0.001396	0.001182	0.001042	0.000877	0.000747	0.000594
0.001261	0.001088	0.000961	0.000824	0.000681	0.000565
0.001133	0.000998	0.000860	0.000695	0.000606	0.000573
0.000999	0.000913	0.000755	0.000619	0.000562	0.000516
0.000855	0.000743	0.000662	0.000609	0.000533	0.000473
0.000789	0.000688	0.000607	0.000546	0.000471	0.000429
0.000710	0.000664	0.000561	0.000495	0.000436	0.000402
0.000629	0.000587	0.000517	0.000464	0.000433	0.000391
0.000554	0.000506	0.000482	0.000450	0.000428	0.000393
0.000488	0.000484	0.000434	0.000455	0.000388	0.000386
0.000482	0.000457	0.000420	0.000399	0.000372	0.000371
0.000461	0.000426	0.000399	0.000384	0.000378	0.000368
0.000416	0.000395	0.000394	0.000390	0.000380	0.000396
0.000405	0.000401	0.000395	0.000365	0.000348	0.000374
0.000407	0.000400	0.000370	0.000348	0.000365	0.000352
0.000384	0.000379	0.000369	0.000379	0.000354	0.000349
0.000363	0.000363	0.000358	0.000382	0.000362	0.000358
0.000364	0.000376	0.000358	0.000367	0.000342	0.000354
0.000349	0.000365	0.000371	0.000371	0.000336	0.000355
0.000350	0.000341	0.000353	0.000361	0.000366	0.000342
0.000353	0.000335	0.000351	0.000361	0.000363	0.000340
0.000364	0.000359	0.000367	0.000373	0.000359	0.000340
0.000361	0.000357	0.000365	0.000341	0.000345	0.000346
0.000338	0.000341	0.000366	0.000366	0.000358	0.000336
0.000343	0.000335	0.000366	0.000372	0.000359	0.000325

Table A. 4: Energy of Townsville Cont'd

24	25	26	27	28	29
0.001050	0.000934	0.000822	0.000764	0.000810	0.001020
0.000777	0.000650	0.000540	0.000484	0.000447	0.000435
0.000728	0.000622	0.000474	0.000437	0.000431	0.000422
0.000663	0.000624	0.000501	0.000455	0.000451	0.000406
0.000612	0.000563	0.000488	0.000452	0.000433	0.000419
0.000631	0.000522	0.000481	0.000407	0.000408	0.000416
0.000568	0.000500	0.000468	0.000404	0.000428	0.000411
0.000572	0.000472	0.000419	0.000425	0.000414	0.000384
0.000582	0.000471	0.000402	0.000395	0.000366	0.000367
0.000529	0.000437	0.000384	0.000386	0.000367	0.000378
0.000496	0.000410	0.000361	0.000405	0.000381	0.000382
0.000460	0.000407	0.000398	0.000402	0.000384	0.000359
0.000433	0.000395	0.000387	0.000377	0.000355	0.000351
0.000410	0.000394	0.000387	0.000367	0.000358	0.000364
0.000385	0.000383	0.000396	0.000375	0.000353	0.000361
0.000393	0.000374	0.000357	0.000355	0.000347	0.000345
0.000379	0.000360	0.000353	0.000353	0.000355	0.000343
0.000360	0.000381	0.000391	0.000360	0.000356	0.000352
0.000369	0.000372	0.000388	0.000357	0.000350	0.000328
0.000369	0.000368	0.000348	0.000341	0.000331	0.000344
0.000376	0.000354	0.000363	0.000365	0.000363	0.000356
0.000363	0.000371	0.000366	0.000350	0.000361	0.000359
0.000361	0.000366	0.000353	0.000335	0.000360	0.000367
0.000342	0.000336	0.000346	0.000341	0.000359	0.000354
0.000353	0.000345	0.000355	0.000361	0.000366	0.000364
0.000358	0.000329	0.000365	0.000356	0.000357	0.000371
0.000364	0.000348	0.000375	0.000338	0.000336	0.000346
0.000354	0.000359	0.000378	0.000370	0.000367	0.000372
0.000347	0.000348	0.000352	0.000350	0.000348	0.000360
0.000362	0.000356	0.000334	0.000348	0.000334	0.000356
0.000354	0.000360	0.000346	0.000345	0.000334	0.000339
0.000366	0.000354	0.000366	0.000354	0.000369	0.000369
0.000364	0.000337	0.000351	0.000327	0.000333	0.000354

Table A. 4: Energy of Townsville Cont'd

30	31	32
0.000961	0.000795	0.000759
0.000445	0.000465	0.000435
0.000401	0.000411	0.000409
0.000398	0.000402	0.000391
0.000389	0.000392	0.000422
0.000383	0.000364	0.000408
0.000399	0.000380	0.000384
0.000379	0.000364	0.000351
0.000375	0.000362	0.000363
0.000386	0.000377	0.000362
0.000391	0.000379	0.000372
0.000371	0.000386	0.000368
0.000373	0.000388	0.000358
0.000370	0.000366	0.000378
0.000355	0.000353	0.000363
0.000320	0.000352	0.000338
0.000316	0.000363	0.000341
0.000346	0.000324	0.000340
0.000334	0.000328	0.000347
0.000315	0.000348	0.000357
0.000350	0.000342	0.000355
0.000364	0.000353	0.000335
0.000376	0.000367	0.000341
0.000350	0.000366	0.000366
0.000365	0.000349	0.000375
0.000365	0.000351	0.000363
0.000362	0.000377	0.000366
0.000357	0.000391	0.000366
0.000336	0.000362	0.000365
0.000374	0.000356	0.000337
0.000349	0.000332	0.000312
0.000345	0.000325	0.000342
0.000348	0.000339	0.000350

## Appendix B: Source Codes

### CreateExamples.m

```
%% 7 Channel
% % function CreateExample
%
% filename = uigetfile('*.*','Select an image file');;
%
% figure(100)
% I=imread(filename);
% imagesc(I);
% axis off
% axis image
% axis fill
% [x,y]=ginput(1);
% x=round(x);
% y=round(y);
% hold on
% plot([x-64 x-64],[y-64 y+63],'r-','linewidth',2);
% plot([x+63 x+63],[y-64 y+63],'r-','linewidth',2);
% plot([x-64 x+63],[y-64 y-64],'r-','linewidth',2);
% plot([x-64 x+63],[y+63 y+63],'r-','linewidth',2);
% hold off
% set(gca,'position',[0 0 1 1],'units','normalized')
% print(['.\Archive\' filename(1:end-4) '_with_ROI'],'-djpeg');
% J=rgb2gray(I(y-64:y+63,x-64:x+63,:));
% J=double(J);
%
% figure
% imagesc(J);
% colormap(gray(256));
% axis off
% axis tight
% axis fill
% set(gca,'position',[0 0 1 1],'units','normalized')
% print(['.\Archive\' filename(1:end-4) '_ROI_gray'],'-djpeg');
%
%
% load('FB_7channel_best_freq_localized.mat');
% [power_J,decomposed_J]=fb_image_decomposition(J,w);
% write_power_file(['.\Archive\' filename(1:end-4) '.txt'],power_J);

% kmPerSample=noPixel/km;
%% 33 Channel
% function CreateExample
```

```

filename = uigetfile('*.*','Select an image file');;

figure(100)
I=imread(filename);
imagesc(I);
axis off
axis image
axis fill
[x,y]=ginput(1);
x=round(x);
y=round(y);
hold on
plot([x-256 x-256],[y-256 y+255],'r-','linewidth',2);
plot([x+255 x+255],[y-256 y+255],'r-','linewidth',2);
plot([x-256 x+255],[y-256 y-256],'r-','linewidth',2);
plot([x-256 x+255],[y+255 y+255],'r-','linewidth',2);
hold off
set(gca,'position',[0 0 1 1],'units','normalized')
print(['.\Archive\' filename(1:end-4) '_with_ROI'],'-djpeg');
J=rgb2gray(I(y-256:y+255,x-256:x+255,:));
J=double(J);

figure
imagesc(J);
colormap(gray(256));
axis off
axis tight
axis fill
set(gca,'position',[0 0 1 1],'units','normalized')
print(['.\Archive\' filename(1:end-4) '_ROI_gray'],'-djpeg');

load('FB_33channel_best_freq_localized.mat');
[power_J,decomposed_J]=fb_image_decomposition(J,w);
write_power_file(['.\Archive\' filename(1:end-4) '.txt'],power_J);

% kmPerSample=noPixel/km;

```

### **fb\_image\_decomposition.m**

```
function [power_J,J]=fb_image_decomposition(I,w)
% function J=fb_decomposition(I,w);

[K L]=size(w);
for i=1:K
    w(i,:)=w(i,:)/sqrt(w(i,:)*w(i,:)');
end
[N M]=size(I);
ave=sum(sum(I))/(N*M);
I=I - ave;
J=zeros(K,K,N,M);
for i=1:K
    for j=1:K
        J(i,j,:,:)=conv2(w(i,:),w(j,:),I,'same');
    end
end

J=J(:,:,1:K:N,1:K:M);

power_J=zeros(K,K);

for i=1:K
    for j=1:K
        power_J(i,j)=sum(sum(abs(squeeze(J(i,j,:,:)))));
    end
end
power_J=power_J./(N*M);
power_J(1,1)=0;
```

### **write\_power\_file.m**

```
function write_power_file(filename,power_J)
M=max(max(power_J));
[max_row,max_col]=find(M==power_J)

[N M]=size(power_J);

fid=fopen(filename,'w');
fprintf(fid,'%d,%d \r\n',max_row-1,max_col-1);
for i=1:N
    fwrite(fid,num2str(i-1),'char');
    fprintf(fid,' &');
    for j=1:M
        temp=num2str(power_J(i,j));
        L=length(temp);
        L=min([L 6]);
        for l=1:L
            fwrite(fid,temp(l),'char');
        end
        if j~=M
            fprintf(fid,' &');
        end
    end
    fprintf(fid,' \\\\ \r\n');
end
fclose(fid);
```

**computeFreq.m**

```
function [hortFreq vertFreq]=computeFreq(max_row,max_col,Fs,L)  
BW=Fs/(2*L);  
hortFreq=(max_row+0.5)*BW;  
vertFreq=(max_col+0.5)*BW;
```